

INVESTIGATIONS OF CARBON AND WATER FLUXES IN A SIERRA NEVADA
MEADOW

A Thesis submitted to the faculty of
San Francisco State University
in partial fulfillment of
the requirements for
the Degree

Master of Arts

In

Geography: Resource Management and Environmental Planning

by

Darren Alden Blackburn

San Francisco, California

August 2017

Copyright

by

Darren Alden Blackburn

2017

CERIFICATION OF APPROVAL

I certify that I have read Investigations of carbon and water fluxes in a Sierra Nevada meadow by Darren Alden Blackburn, and that in my opinion this work meets the criteria for approving a thesis submitted in partial fulfillment of the requirement for the degree Master of Arts in Geography: Resource Management and Environmental Planning at San Francisco State University.

Andrew Oliphant, Ph.D.

Professor of Geography & Environment

Jerry Davis, Ph.D.

Professor of Geography & Environment

INVESTIGATIONS OF CARBON AND WATER FLUXES IN A SIERRA NEVADA
MEADOW

Darren Alden Blackburn

San Francisco, California

2017

This study investigates the diurnal and seasonal surface-atmosphere exchanges of carbon dioxide (CO_2), water and energy in a partly degraded Northern Sierra Nevada meadow. The eddy covariance technique was employed to quantify these exchanges in Loney Meadow (1822 m a.s.l.) for most of the annual snow-free period from May to September 2016. This meadow impacted by stream channel incision and is scheduled to undergo restoration work to raise the water table. The observed net ecosystem exchange (NEE) of CO_2 showed that the ecosystem functioned as a strong sink throughout most of the study period sequestering an average of $-18.51 \text{ gC m}^{-2} \text{ d}^{-1}$ during the peak of the growing season. The entire study period produced an average daily total NEE value of $-7.71 \text{ gC m}^{-2} \text{ d}^{-1}$. The meadow progressed from a strong sink in the peak of the growing season ($-18.51 \text{ gC m}^{-2} \text{ d}^{-1}$) to a weak source ($2.97 \text{ gC m}^{-2} \text{ d}^{-1}$) following a decline in soil moisture. During daylight hours, photosynthetically active radiation (PAR) was shown to be the dominant driver of the CO_2 flux with values ranging between -0.2 and $-1.0 \text{ mgC m}^{-2} \text{ s}^{-1}$. At night, GPP shut down and the ecosystem functioned as a small source of CO_2 with values ranging between 0.1 and $0.3 \text{ mgC m}^{-2} \text{ s}^{-1}$. At the seasonal scale soil moisture was shown to be a strong control on the CO_2 exchange, which has important implications for understanding the impact of land management and climate change on meadow carbon budgets.

I certify that the Abstract is a correct representation of the content of this thesis.

Chair, Thesis Committee

Date

ACKNOWLEDGEMENTS

Thank you so much to my committee, Andrew Oliphant and Jerry Davis. The knowledge, adventures and support you have given me throughout this journey is truly appreciated. I have had the pleasure of getting to know a number of the Geography Department's faculty and lecturers, so thank you to them for their guidance and advice. Thank you, Sara Baguskas, for sharing your enthusiasm and for taking the time to talk about my project and discuss future opportunities. Thanks to Rachel Hutchinson and the team at SYRCL for collaborating with us and facilitating access to the study site. To my meadow buddy, Austen Lorenz, thanks for talking meadows with me and always being fun to work with. Thanks to Quentin Clark for support in the field and in the Map Library (including Sweatpants Saturdays). Suzanne Maher, thank you for motivating me to take on this project and for all the help along the way. Christa Meier, as a fellow struggling climatologist, thank you for always being ready with kind words and occasional commiseration. My roommate from UCLA, Ryon Nixon, thanks for giving me friendship, energy and clarity when I really needed it. Yael Golan, Tov! Thank you for always being willing to take breaks with me and providing me with dog-sitting opportunities. Kerstin Kalchmayr for the hikes, Charlotte Hummer for the laughs, Danielle Mazzella for the drinks, and to the rest of my fellow graduate students, thanks! Finally, a big thank you to Loney Meadow! It will always be a special place to me.

TABLE OF CONTENTS

List of Tables	viii
List of Figures	ix
1.0 INTRODUCTION	1
1.1 Research Objective	2
1.2 Sierra Nevada Mountain Meadows	2
1.3 Healthy vs. Degraded Meadows	7
1.4 Restoration of Meadows	12
2.0 STUDY SITE DESCRIPTION	13
3.0 METHODS	18
3.1 Eddy Covariance Theory	18
3.2 Experimental Design	20
3.3 Data Processing, Rejection and Uncertainty	22
3.3.1 Plausible Limit Testing	22
3.3.2 Insufficient Turbulence	23
3.3.3 Footprint Assessment	24
3.4 Partitioning and Gap Filling CO ₂ Exchanges	25
3.5 Accuracy Assessment: Energy Balance Closure	27
4.0 RESULTS	31
4.1 Observed Net Ecosystem Exchange of CO ₂	31

4.1.1 Diurnal Patterns of Net Ecosystem Exchange	32
4.1.2 Seasonal Patterns of CO ₂ Exchanges	34
4.2 CO ₂ Flux Partitioning into RE and GPP	36
4.2.1 Ecosystem Respiration	37
4.2.2 GPP and Light Use Efficiency	40
4.3 Diurnal Controls on Ecosystem CO ₂ Exchange	42
4.4 Seasonal and Synoptic Controls on Ecosystem CO ₂ Exchange	46
5.0 DISCUSSION.....	50
5.1 Annual CO ₂ Budget Estimate	51
5.2 Comparison of Loney Meadow to Wetland and Grassland Ecosystems.....	54
5.2.1 Comparison of Diurnal Patterns and Daily Totals	56
5.2.2 Annual Comparison.....	58
5.3 Unmeasured Carbon Fluxes in Loney Meadow	60
5.3.1 Methane Flux.....	61
5.3.2 Transport of Dissolved Organic Carbon through Stream Network	62
5.3.3 Grazing by Livestock	63
5.3 Implications for Meadow CO ₂ Exchanges under Changing Land-use and Climate.....	64
6.0 CONCLUSIONS	66
7.0 REFERENCES	69

LIST OF TABLES

Table	Page
1. Dominant species commonly associated with three plant communities found in SN mountain meadows.....	5
2. Total snowfall recorded at Bowman Dam, CA (Elevation: 1643 m) for the 2014-15 and 2015-16 water years. Source: WRCC 2017.....	14
3. Energy balance closure statistics using linear regression after applying testing criteria to flux data.....	31
4. Growing season phases identified with date ranges, descriptions, images of the meadow surface and environmental conditions.....	36
5. Regression parameters and statistics for the respiration model using binned averages and divided into seasonal periods (1-4) and the entire study period (ALL) with average observed nighttime RE.....	39
6. LUE curve parameters and statistics with average observed GPP.....	41
7. The average daily CO ₂ flux values for each seasonal period and the entire study period.....	46
8. Annual CO ₂ budget estimates divided into observed seasonal periods (1-4), modeled periods (0 and 5) and the estimated flux when snow covered the meadow.....	53
9. Comparison of Loney Meadow's estimated net annual CO ₂ exchange to wetland and grassland ecosystems.....	59

LIST OF FIGURES

Figures	Page
1. Images of Loney Meadow showing the meadow plant community at four distinct phases of the seasonal cycle.....	7
2. Ecological process schematic of a healthy mountain meadow. From American Rivers (2012).....	9
3. Ecological process schematic of an unhealthy mountain meadow. From American Rivers (2012).....	11
4. Climate normal data for Bowman Dam, CA (1643 m a.s.l.) compiled with data spanning from 6/01/1896 to 05/31/2016. The shaded area represents the approximate.....	15
5. Visible satellite image of Loney Meadow during the summer and extent indicator within California. Source: Esri, DigitalGlobe, GeoEye, Earthstar Geographics, CNES/Airbus DS, USDA, USGS, AeroGRID, IGN, and the GIS User Community.....	16
6. Table of equipment specifications (left) and image of the flux tower deployed at Loney Meadow (right).....	21
7. Energy balance closure for all good data with turbulent fluxes on the y-axis and available energy on the x-axis.....	29
8. Diurnal 30-minute ensemble averages of NEE at Loney Meadow with error bars representing +/- one standard for the entire observation period. The shaded arc represents the cosine of the solar zenith angle (Z) for minimum and maximum solar declination during the observation period.....	32

9. Daily total NEE for the entire study period (bottom). Selected images of meadow surface (west facing) taken from the top of the flux tower and approximation of distinct phases of the growing season divided into four periods (top).....	34
10. Soil temperature response of nocturnal respiration with binned average temperature in 1°C increments.....	38
11. LUE curves for the total study period and separated into four seasonal periods.....	41
12. Diurnal ensemble 30-minute averages of GPP (a), RE (b), PAR (c), soil temperature (Ts) (d), vapor pressure deficit (VPD) (e), and volumetric water content (VWC) (f) according to seasonal period.....	44
13. Daily total CO ₂ exchanges between the meadow surface and the atmosphere throughout the growing season (a) and (in descending order) environmental controls including daily average photosynthetically active radiation (PAR) (b), air/soil temperature (c), daily total precipitation (c) and soil moisture (d). Selected images (top) of meadow surface (west facing) taken from the top of the flux tower and approximation of distinct phases of the growing season divided into four periods.....	47
14. Linear regression of daily total CO ₂ flux data for seasonal Periods 1 and 4.....	52

1.0 INTRODUCTION

Mountain meadows are important environmental systems at the headwaters of Sierra Nevada (SN) river catchments. Viers et al. (2013) estimate that there about 17,039 meadows in the SN covering about 77,659 hectares of land and, although they account for small percentage of land cover (~0.01%), meadows support a diverse range of species and provide invaluable services to human populations (Kattelmann and Embury 1996; Fites-Kaufman et al. 2007; Norton et al. 2011 Viers et al. 2013). Previous research has shown that meadows perform important environmental functions such as moderating seasonal flow patterns, hosting abundant mesic/hydric plant species, filtering sediments etc., making them integral components of the mountain hydrologic regime (Loheide et al. 2009; Lowry et al. 2011; Viers et al. 2013). Meadows are sensitive to land use changes and many of these ecological processes may have been altered as a result (Ratliff 1982; Kattelmann and Embury 1996; Purdy and Moyle 2006; Loheide and Gorelick 2007). The impacts of climate change have generated an increase in studies that investigate carbon cycling in meadows. These studies have primarily focused on carbon stocks from biometric estimates (Norton et al. 2011) but much less is known about the rates of CO₂ exchange, its seasonal evolution and main environmental controls (Fites-Kaufman et al. 2007).

1.1 Research Objective

The objective of this project is to investigate ecosystem-atmosphere CO₂ exchanges of a partly degraded montane meadow at an elevation of 1,822 m (Loney Meadow) in the Northern Sierra Nevada. In particular, this research assesses the seasonal patterns of ecosystem functioning and the environmental controls on CO₂ exchange. To achieve these objectives, a micrometeorological approach using the eddy covariance technique was employed at the study site to directly measure the exchange of CO₂, water vapor and energy between the surface and the atmosphere throughout the growing season at a 30-minute frequency. This approach is widely used around the world assessing ecosystems (e.g. Baldocchi 2008; Oliphant 2012), but very few have focused on mountain meadows.

1.2 Sierra Nevada Mountain Meadows

Meadows can be identified and classified according to their hydrogeomorphic properties and soil/vegetation profiles. In terms of hydrology, they can act as sources (outflow), sinks (inflow) or pass-through systems (throughflow) for water (Weixelman et al. 2011). In general, SN meadows are found at elevations greater than 500 m, dominated by herbaceous species supporting plants that use surface/shallow groundwater (depth < 1 m) with finely textured surficial soils (Viers et al. 2013). They are typically considered seasonal wetlands or semiwetlands that depend on runoff from snowmelt, which sustain surface and subsurface flows that subsequently maintain high groundwater levels (Ratliff

1985; Loheide et al. 2009). There is a significant amount of diversity among SN meadows resulting in a wide range of classifications (e.g. riparian, depressional, wet, mesic, dry, montane, alpine, etc.) based on geomorphology, surface/subsurface hydrology, soil characteristics, vegetation patterns and elevation (Ratliff 1985; Holland 1986; Allen 1987; Dwire et al. 2006). However, a shallow groundwater table is the most important factor that links this broad range of classifications together because it sustains high soil moisture levels, which supports the characteristic graminoid and herbaceous species found in meadows (Fites-Kaufman et al. 2007; Loheide et al. 2009).

Vegetation in wet/moist meadows typically consists of hydric and mesic species such as perennial grasses, wet sedges, forbs, and other herbaceous species (Ratliff 1985; Allen 1987; Lowry et al. 2011; Maher 2015). Dry meadows are dominated by more xeric species like perennial grasses and sagebrush and exhibit less overall species richness compared to wet/mesic areas (Allen 1987; Lowry et al. 2011; Maher 2015). Table 1 shows a list of indicator species derived from five vegetation surveys with study sites on both the eastern and western sides of the SN. In general, plant productivity of meadow ecosystems varies most significantly with changes in soil moisture and elevation with mesic communities being the most productive (Ratliff 1985; Fites-Kaufman et al. 2007; Loheide and Gorelick 2007). Vegetation patterns are not highly variable among meadow classifications and types; they also tend to show a gradient of change across the meadow surface. Spatial distribution patterns of vegetation is usually consistent with changes in the water table across the meadow surface with the more water dependent species located

closer to the water sources (Lowry et al. 2011). The spatial patterns of vegetation within individual meadows is indicative of an extensive land-water ecotone driven by soil moisture gradients (Kondolf et al. 1996).

Table 1. Dominant species commonly associated with three plant communities found in SN mountain meadows.

Scientific Name	Common Name	Source
Wet Meadow		
<i>Aster alpinus</i>	alpine aster	Lowry et al. 2011
<i>Carex aquatilis</i> Wahl	water sedge	Dwire et al. 2006
<i>Carex nebrascensis</i>	Nebraska Sedge	Maher 2015; Fites-Kaufman et al. 2007
<i>Carex subnigricans</i>	nearlyblack sedge	Lowry et al. 2011
<i>Carex utricularata</i>	Northwest Territory sedge	Maher 2015
<i>Carex vesicaria</i>	blister sedge	Lowry et al. 2011; Fites-Kaufman et al. 2007
<i>Dodecatheon alpinum</i>	alpine shooting star	Lowry et al. 2011
<i>Horkelia fusca</i>	pinewoods horkelia	Lowry et al. 2011
<i>Polygonum bistortoides</i>	American bistort	Lowry et al. 2011
<i>Ptilagrostis kingii</i>	Sierra false needlegrass	Lowry et al. 2011
<i>Ranunculus repens</i>	creeping buttercup	Maher 2015
<i>Salix eastwoodiae</i>	mountain willow	Lowry et al. 2011
<i>Stellaria longipes</i>	longstalk starwort	Lowry et al. 2011; Fites-Kaufman et al. 2007
<i>Trisetum spicatum</i>	northern oat grass	Lowry et al. 2011
Mesic/Moist Meadow		
<i>Antennaria corymbosa</i>	flat-top pussietoes	Lowry et al. 2011
<i>Calamagrostis breweri</i>	shorthair reedgrass	Lowry et al. 2011
<i>Carex microptera</i>	smallwing sedge	Dwire et al. 2006
<i>Carex nevadensis</i>	Little green sedge	Maher 2015
<i>Castilleja leonii</i>	Lemmon's Indian paintbrush	Lowry et al. 2011
<i>Cirsium scariosum</i>	meadow thistle	Debinski et al. 2010
<i>Deschampsia caespitosa</i>	Tufted hair grass	Maher 2015; Fites-Kaufman et al. 2007; Dwire et al. 2006
<i>Juncus balticus</i>	Baltic rush	Maher 2015; Lowry et al. 2011; Fites-Kaufman et al. 2007; Dwire et al. 2006
<i>Lupinus argenteus</i>	Silvery lupine	Debinski et al. 2010
<i>Perideridia bolanderi</i>	Bolander's yampah	Maher 2015
<i>Phleum alpinum</i>	Alpine timothy	Maher 2015
<i>Poa pratensis</i>	Kentucky bluegrass	Fites-Kaufman et al. 2007; Dwire et al. 2006
<i>Potentilla gracilis</i>	slender cinquefoil	Debinski et al. 2010
<i>Solidago multiaadata</i>	alpine goldenrod	Lowry et al. 2011
<i>Trifolium longipes</i>	Longstalk clover	Maher 2015; Dwire et al. 2006
<i>Vaccinium caeserpitum</i>	dwarf bilberry	Lowry et al. 2011
Dry Meadow		
<i>Artemisia tridentata</i>	big sagebrush	Maher 2015; Debinski et al. 2010; Lowry et al. 2011
<i>Bromus tectorum</i>	cheatgrass	Maher 2015
<i>Carex douglasii</i>	Douglas' sedge	Fites-Kaufman et al. 2007
<i>Carex filifolia</i>	threadleaf sedge	Lowry et al. 2011
<i>Carex rossii</i>	Ross' sedge	Lowry et al. 2011
<i>Danthonia californica</i> Boland.	California oat grass	Dwire et al. 2006
<i>Muhlenbergia richardsonis</i>	mat muhly	Fites-Kaufman et al. 2007
<i>Pinus contorta</i>	lodgepole pine	Lowry et al. 2011
<i>Poa bulbosa</i>	bulbous bluegrass	Maher 2015
<i>Poa secunda</i>	pine bluegrass	Fites-Kaufman et al. 2007
<i>Purshia tridentata</i>	Antelope bitterbrush	Maher 2015

Mountain meadows exhibit strong seasonality with annual growth cycles that emerge in the late spring as snowmelt increases runoff and they begin to senesce in the late summer as the water table drops and soil moisture in the root zone gets depleted (Loheide and Gorelick 2007). Figure 1 shows a chronosequence of pictures of Loney Meadow surface highlighting the strong seasonal contrast from vegetation-free snowpack to rapid spring and early summer growth, with senescence evident in late summer. Similar to grassland ecosystems, senescence is typically associated with decline in water availability occurring in the summer and fall months until snow covers the meadow surface again in the winter (Flanagan et al. 2002; Loheide and Gorelick 2007; Scott et al. 2010). The timing of spring snowmelt, peak streamflow, snow cover and the relative seasonal snow water equivalent (SWE) in the SN are influenced by interannual and decadal-scale climate variability, in particular large scale temperature patterns (Hamlet et al. 2005; Stewart et al. 2005). In general, over the past five decades, the timing of spring streamflow in western North America has experienced a shift so that peak flow is arriving one or two weeks earlier with less precipitation falling as snow (Stewart et al. 2005). This shift has been attributed to warming temperature trends that tend to reduce the amount of precipitation falling as snow as well as generate earlier spring snowmelt (Stewart et al. 2005; Lowry et al. 2011; Viers and Rheinheimer 2011). Annual SWE directly influences soil moisture content in meadows as the growing season progresses, with water levels near field capacity in the early spring and dropping significantly in the summer when

water levels decline as a function of reduced runoff coming from higher elevations (Lowry et al. 2011).



Figure 1. Images of Loney Meadow showing the meadow plant community at four distinct phases of the seasonal cycle.

1.3 Healthy vs. Degraded Meadows

Because of their geomorphic characteristics that disperse and store water sourced from the SN snowpack, meadows act as a network of natural cascading reservoirs that

provide a number of important ecological benefits to downstream ecosystems and communities. They attenuate flood flows, sustain base flows and promote groundwater recharge by dispersing water across the low gradient floodplain (Kattelmann and Embury 1996; Lowry et al. 2011; Viers et al. 2013). In addition to supporting a diverse range of plant species, they provide critical habitat to a number of bird, invertebrates, fish and other wildlife (Kattelmann and Embury 1996; Purdy and Moyle 2006). They improve water quality by filtering sediment and the densely rooted vegetation improve bank stability and reduce erosion along stream channels (Ratliff 1982; Loheide and Gorelick 2007). A diagram summarizing the ecological processes of a healthy riparian meadow is presented in Figure 2. However, these processes vary based on the classifications and subtypes mentioned previously. The capacity of mountain meadow ecosystems to provide these benefits is primarily linked to the naturally occurring high water table and the subsequent seasonal progression of soil moisture levels (Allen-Diaz 1991; Fites-Kaufman et al. 2007; Loheide et al. 2009).

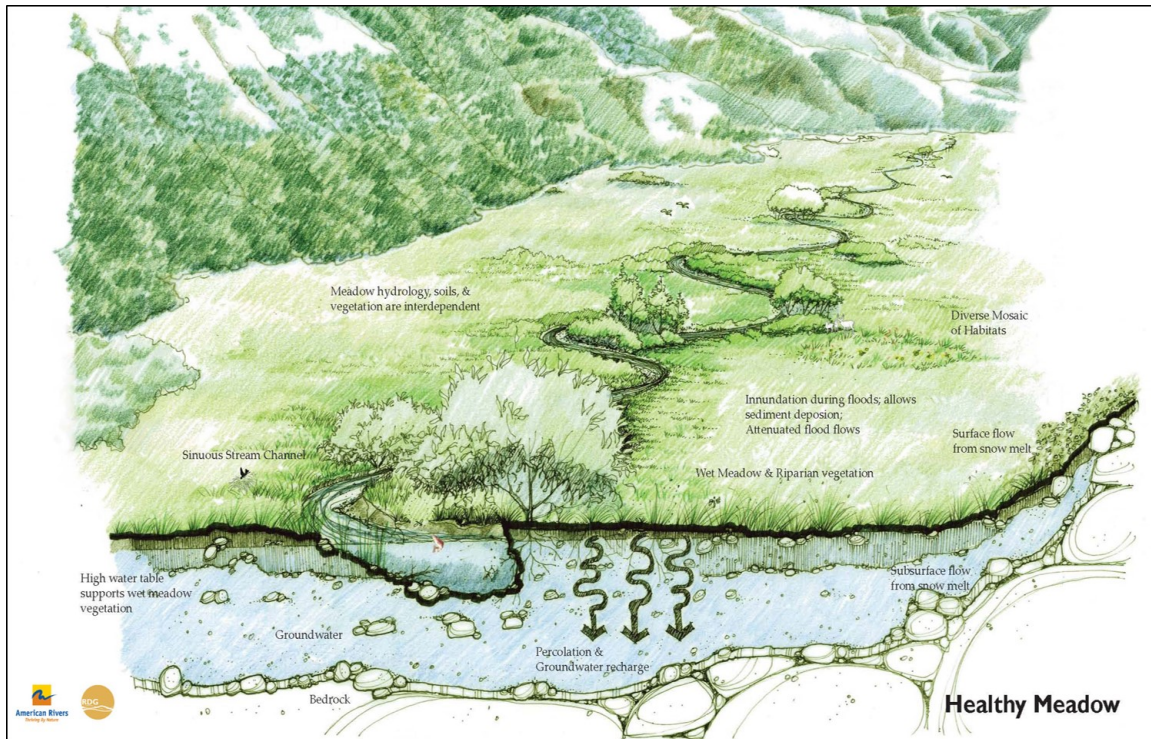


Figure 2. Ecological process schematic of a healthy mountain meadow. From American Rivers (2012).

Historic and current land use in the Sierra Nevada have contributed to processes that negatively affect the ability of mountain meadows to function as described above (Ratliff 1985; Kattelmann and Embury 1996; Purdy and Moyle 2006; Viers et al. 2013; Lowry et al. 2011; Weixelman et al. 2011). Previous research indicates that historical overgrazing by sheep and cattle are a primary source of degradation in SN meadows (Purdy and Moyle 2006; Viers et al. 2013). Logging, mining, development (e.g. rail and road building) have also been identified as sources of degradation (Loheide and Gorelick 2007). These activities affect the meadow hydrology by increasing runoff from the watershed above the meadow and in many cases divert or straighten channels (Purdy and

Moyle 2006). These alterations in turn enhance stream channel incision and reduce meandering patterns that distribute water across the meadow surface. This leads to a lowering of the water table within the meadow (Figure 3) (Viers et al. 2013). Channel incision disconnects the stream channel with the meadow surface thus draining the stored water and decreasing the meadows ability to store water and sustain native vegetation (Viers et al. 2013; Loheide et al. 2009). The subsequent change in water table position and the disruption to natural flow patterns has been shown to reduce overall soil water content in the root zone of meadow, which impacts the productivity and distribution of vegetation (Figure 3) (Kattelmann and Embury 1996; Loheide et al. 2009; Lowry et al. 2011).

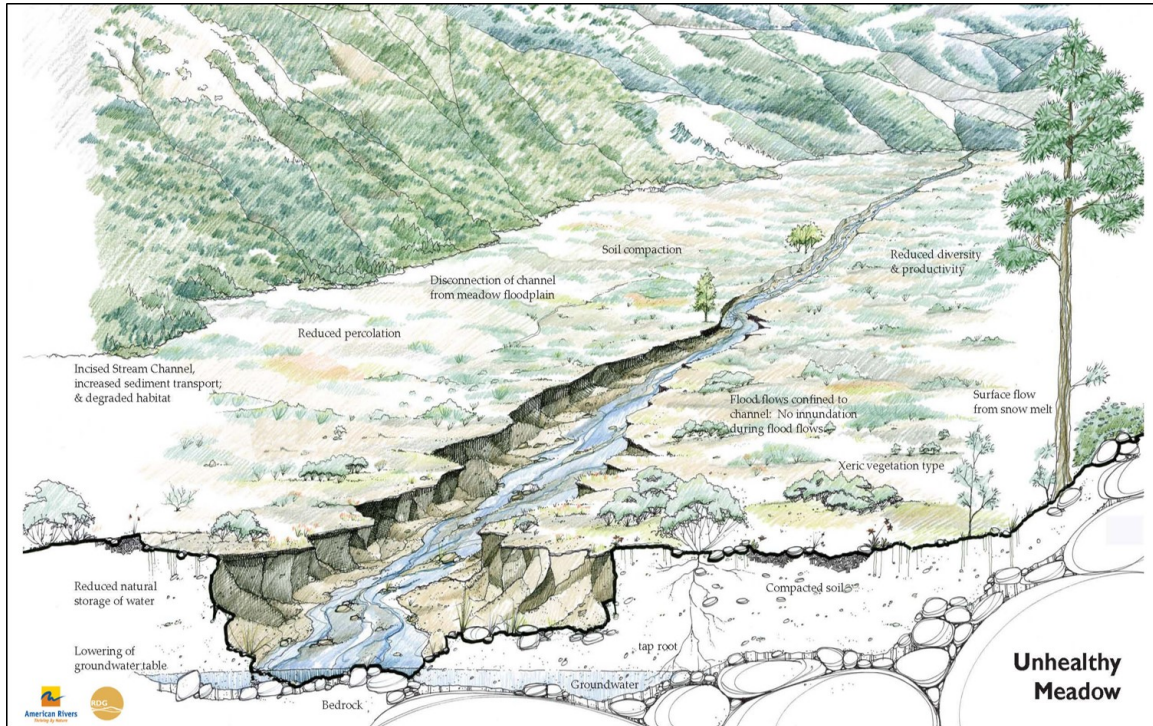


Figure 3. Ecological process schematic of an unhealthy mountain meadow. From American Rivers (2012).

The impact of degradation on vegetation patterns tends to be a succession from the native hydric/mesic species to more xeric species commonly associated with dryland meadows (Table 1) (Allen-Diaz 1991; Loheide and Gorelick 2007; Loheide et al. 2009; Pope et al. 2015). Previous studies have linked water availability in meadows to fluctuations in species richness/percent cover, vulnerability to invasive species encroachment and the capacity to sequester and store greenhouse gases (Dwire et al. 2006; Fites-Kaufman et al. 2007; Haugo and Halpern 2007; Blankenship and Hart 2014; Maher 2015). A comparison of existing measurements of CO₂ fluxes in wetland, grassland and semi-arid ecosystems suggests that hydric/mesic species are much faster

growing and absorb more CO₂ from the atmosphere (e.g. Ratliff 1985; Flanagan et al. 2002; Kayranli et al. 2010; Norton et al. 2011. Xeric species, on the other hand, tend to be weak sinks of CO₂ and limited water conditions (e.g. drought) can cause these types of ecosystems to shift from a net sink to a source of carbon dioxide gas to the atmosphere on an annual basis (Flanagan et al. 2002; Lund et al. 2010; Scott et al. 2010). The relative drying patterns that are a consequence of meadow degradation coupled with increased drought conditions stemming from climate change could potentially generate a positive feedback loop that weakens the ability of mountain meadows in the SN to store carbon (Debinski et al. 2010; Kayranli et al. 2010).

1.4 Restoration of Meadows

Because of the important ecological benefits and services that mountain meadows provide, there has been increased interest in restoring meadows that have been negatively impacted by anthropogenic land use (Loheide and Gorelick 2007; Pope et al. 2015). The most commonly used “rewatering” technique to restore the natural hydrology in meadows is known as pond-and-plug (Hammersmark et al. 2008; Pope et al. 2015). This method consists of excavating alluvial materials from the floodplain and using them to plug the incised channels (Hammersmark et al. 2008). The earthen plug then forces inflowing water to disperse across the meadow surface instead of being flushed out through the degraded channel and reduces stream bank erosion (Hammersmark et al. 2008). Loheide et al. (2009) suggest that, in order to effectively reconnect the stream

channel to the flood plain, about 70% of the regional groundwater flow entering a meadow should occur as basal flux. The goal is to mimic and restore natural processes that raise the volume of subsurface storage by providing a greater spatial opportunity for water to infiltrate (Hammersmark et al. 2008). Like most land management strategies, effective restoration should include ecosystem monitoring before and after the project is executed in order to assess its effectiveness and inform future management decisions.

2.0 STUDY SITE DESCRIPTION

Loney Meadow is located at nearly 2,000 m elevation in the Yuba watershed. The specific coordinates for the study site is 39.4210113°N, -120.6549365°W (Figure 5). Loney Meadow experiences mountain Mediterranean climate conditions with warm dry summers and cold wet winters. On average, temperatures near the study site range between about -3 °C during the winter 26 °C in the summer (Figure 4). Local climate normal data shows that snow typically covers the ground from October to May with peak snow depth occurring in March (Figure 4). Precipitation and relative snowpack varies interannually in the SN, which has a direct impact on the volume and timing of runoff throughout the year. On April 1, 2016, the snow water equivalent was 85% of the average indicating that the study period fell within a moderate drought year (Anderson 2016). The 2015-16 water year followed a four-year period of drought in California with the snow water equivalent considerably below average (Anderson 2016). Table 2 compares the

total snowfall recorded at Bowman Dam, CA for the 2014-15 and 2015-16 water years (WRCC 2017). This indicates that, while still a drought year, the SN snowpack that affected the study period was much closer to average levels than the preceding year. With over one hundred years of compiled data, the climograph from Bowman Dam, located approximately 2.4 km north of the study site at about 400 m lower elevation, shows average regional climate patterns that affect Loney Meadow (Figure 4).

Table 2. Total snowfall recorded at Bowman Dam, CA (1643 m a.s.l.) for the 2014-15 and 2015-16 water years. Source: WRCC 2017.

Time (Month)	2014 - 15 Snowfall (cm)	2015 - 16 Snowfall (cm)
Jul	0	0
Aug	0	0
Sep	0	0
Oct	0	0
Nov	2.5	69.9
Dec	63.5	112.5
Jan	0	104.1
Feb	15.2	35.6
Mar	15.2	111.8
Apr	25.4	12.7
May	0	7.6
Jun	0	0
Annual (Jul - Jun)	121.9	454.2

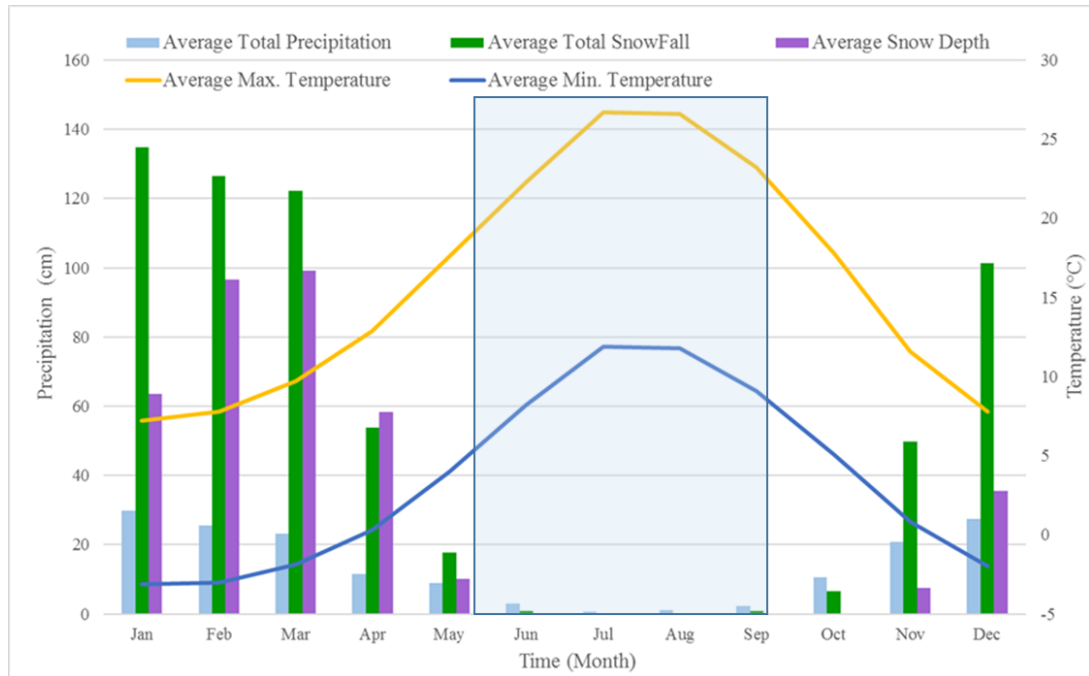


Figure 4. Climate normal data for Bowman Dam, CA (1643 m a.s.l.) compiled with data spanning from 6/01/1896 to 05/31/2016. The shaded area represents the approximate date range that this study took place. Source: WRCC 2017.

Emergent grasses ranging from about 5 – 10 cm high dominated the meadow surface on May 15 with patches of willows (*Salix* spp.) present along the stream channels. During the early spring season, 90 to 100% of the meadow surface was saturated with ponding occurring on over 75% of the surface. In July, leaf area index appeared to reach a maximum at which point vegetation height ranged between 30 and 65 cm. Wildflowers bloomed from mid-May to the end of July containing species such as purple fawn lily (*Erythronium purpurascens*), western buttercup (*Ranunculus* *accidentalis*), Lemmon's yampah (*Perideridia lemmontii*) and common camas (*Camassia* *quamash*) (SYRCL 2017). By September, vegetation height declined to about 20 to 30

cm as the plants senesced. Based on general observations, dominant vegetation types were consistent with the perennial grasses and sedges found in mesic meadows communities described in Table 1.

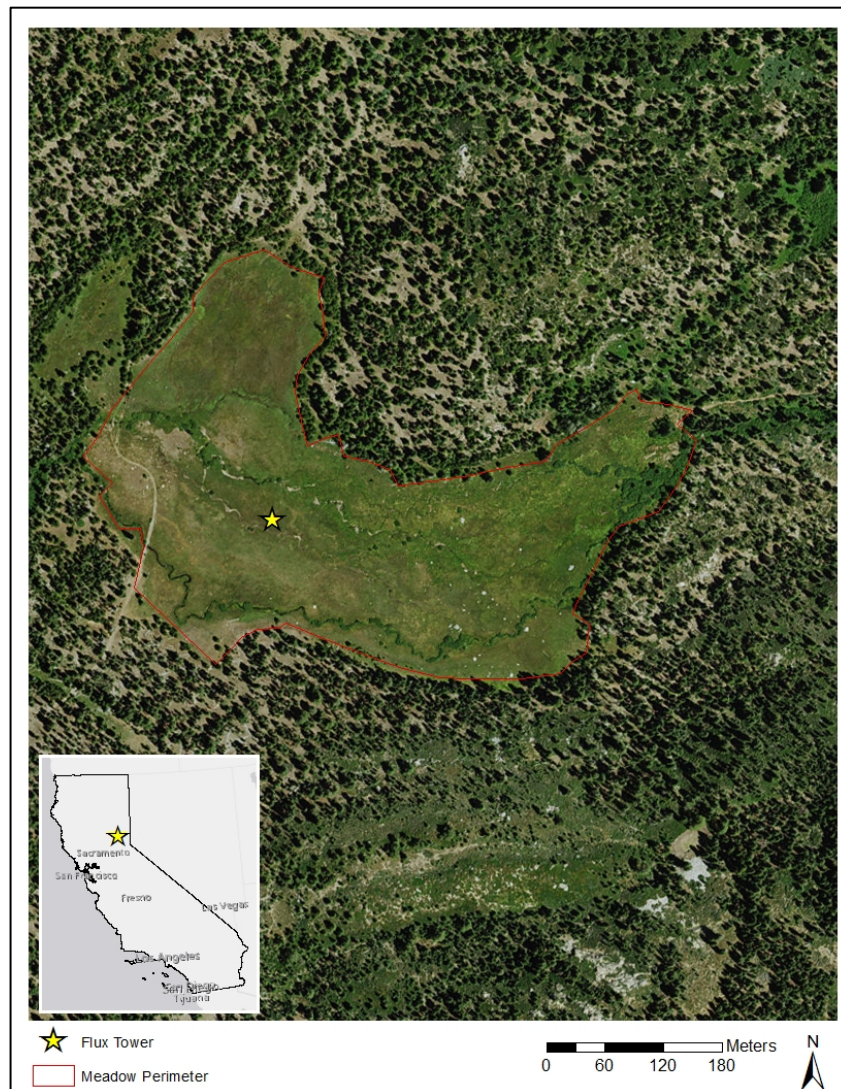


Figure 5. Visible satellite image of Loney Meadow during the summer and extent indicator within California. Source: Esri, DigitalGlobe, GeoEye, Earthstar Geographics, CNES/Airbus DS, USDA, USGS, AeroGRID, IGN, and the GIS User Community.

The meadow contains ephemeral meandering stream channels that are a segment of Texas Creek. The site has an interpretive trail that cuts through the southwestern side of the meadow and it is a popular destination for recreational hiking and bird watching. The area of the meadow is approximately 138,307 m² and is grazed by a herd of about fifty cattle of mixed ages between June and September. The Forest Service (USFS) and National Fish and Wildlife Foundation (NFWF) have identified Loney Meadow as ‘degraded’ and it is scheduled to undergo restoration work to raise the water table in 2017 (Hutchinson 2016). South Yuba River Citizens League (SYRCL) is a non-profit organization that acquired funds to monitor and lead the restoration project. The grant was acquired as part of a larger meadow restoration project funded by the NFWF. The flux tower measurements from this study were incorporated into the pre-restoration monitoring effort by SYRCL. Sections of the river channels and an upstream tributary show evidence of incision but the vegetation shifts described in Section 1.3 have not yet become apparent. Therefore, we identify Loney Meadow as “partly degraded” because vegetation profiles and seasonal productivity will be more similar to that of a healthy meadow with ecological processes resembling Figure 3. The 2017 planned restoration action in Loney Meadow will consist of filling in three sections of the incised channel in order to encourage water dispersal across the floodplain with the goal of maintaining shallow groundwater levels in order to repair any existing damage to the ecosystem and prevent the potential effects of continued degradation.

3.0 METHODS

A micrometeorological research station with eddy covariance instruments (flux tower) was deployed between May 17th and September 6th, 2016. The location of the flux tower near the center of the meadow was selected in order to ensure reasonable fetch during the dominant westerly up-valley winds observed during the day and down-valley drainage flows from the east during the night (Figure 5).

3.1 Eddy Covariance Theory

The eddy covariance method measures ecosystem scale exchanges of trace gasses, momentum and energy between the surface and the atmosphere (Baldocchi 2008; Olliphant 2012). Turbulent eddies in contact with the surface carry properties such as heat and trace gases from the surface into the atmosphere and vice versa (Oke 1987). This exchange is expressed as a flux, which describes how the concentration or quantity of a scalar of interest moves through a unit of area per unit of time (Burba 2013). The instantaneous flux density is calculated by applying Eq. 1, using high frequency measurements of vertical wind speed fluctuations (w') as well as synchronous measurements of fluctuations in the concentration of the scalar (s') of interest (Baldocchi 2003; Aubinet et al. 2012).

$$F_s = \rho_d \overline{w's'} \quad (1)$$

The overbar represents the average covariance between the two atmospheric properties over the averaging period, which is multiplied by the mean air density. For example, carbon dioxide (CO_2) fluxes ($\text{mgC m}^{-2} \text{ s}^{-1}$) are determined by finding the covariance between fluctuations in vertical velocity (m s^{-1}) and the mixing ratio of CO_2 (g kg^{-1}). This equation has been simplified based on the assumptions that air density fluctuations and mean vertical flow are negligible over a reasonably flat and homogenous surface (Burba 2013; Baldocchi 2003). These two requirements constrain the ability of eddy covariance to measure accurately over complex terrain. In this case, we have a fairly homogenous and flat surface immediately being sampled, but one that is surrounded by complex terrain and different vegetation, introducing the potential for local scale processes to influence the observed flux (e.g. Castelvi and Oliphant 2017). Since convective transport occurs very rapidly in nature, the instruments used to measure this covariance need to take precise measurements at high frequency. The typical sampling frequency for EC measurements is 10 Hz or higher and typical averaging periods are 30-minute to one-hour.

Over the averaging period, the source area of the surface that is sampled resembles an elliptical shape extending some distance in the upwind direction. The distance, direction and exact shape of the flux source area (or flux footprint) depends on wind direction, wind speed, surface roughness, atmospheric stability and height of the instruments (Hsieh et al. 2000). EC measurements also require a minimal level of atmospheric turbulence to record exchanges accurately, which varies based on surface

roughness and canopy height (Oliphant 2012). The actual height that EC instruments are mounted also varies based on canopy height and the size of the ecosystem being studied. With an appropriate site selection and deployment of the instrumentation, the EC method provides a rich continuous dataset that describes surface-atmosphere exchanges at the ecosystem scale with high temporal resolution (Baldocchi 2003; Aubinet et al. 2012).

3.2 Experimental Design

The EC and ancillary micrometeorological instrumentation for this study were either mounted on a 3-meter tripod or inserted into the soil substrate nearby. The instruments were wired into a Campbell-Scientific CR3000 data logger and the data was stored on 16 GB SanDisk memory cards. A list of equipment used, variables measured and associated heights are present in Figure 6. Two deep-cycle 12V batteries, charged by a 75 W solar panel, supplied the power to instrumentation. The sampling frequency for this project was 10 Hz and the covariances were averaged over 30-minute periods, as were all ancillary measurements. Both the raw 10 Hz files and 30-minute data were stored on 16 GB SanDisk storage cards. In addition, a Moultrie game camera was attached to the center pole of the tower facing west at a 2.2-meter height. The camera took daily images of the meadow surface at 12:00 P.M.

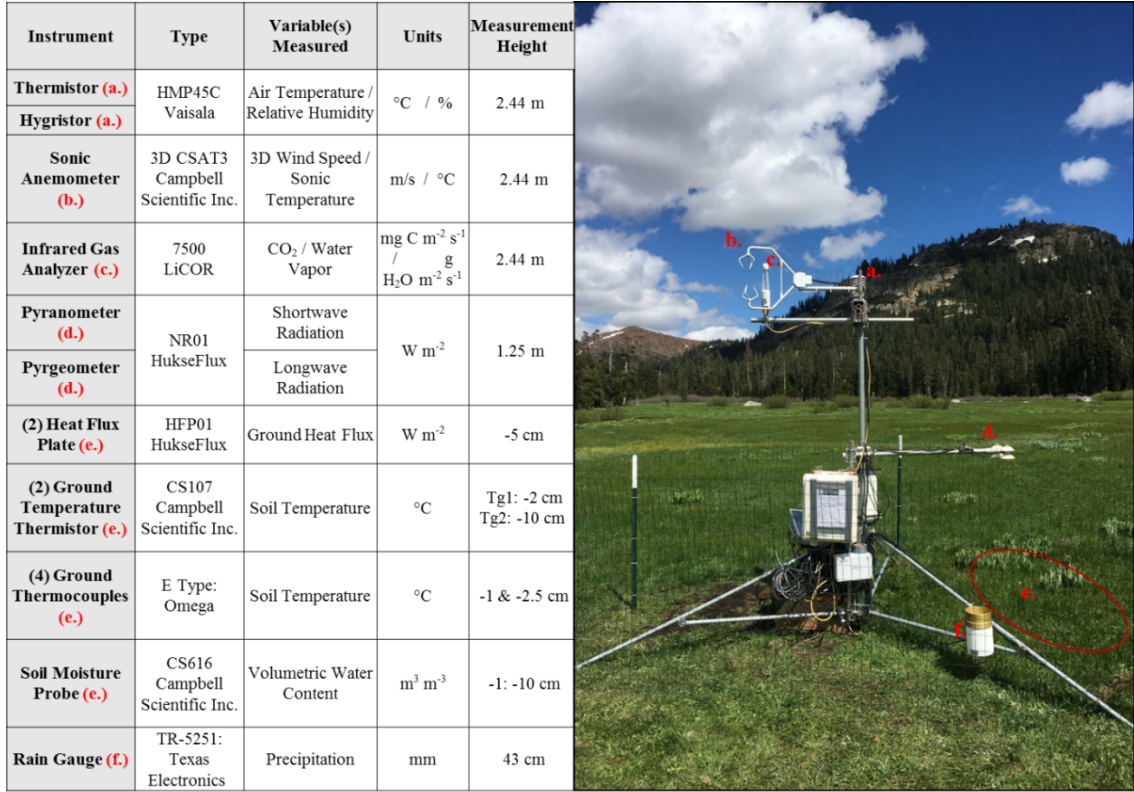


Figure 6. Table of equipment specifications (left) and image of the flux tower deployed at Loney Meadow (right).

A fence was installed around the legs of the flux tower and extended south to enclose an undisturbed area of about four square meters. The intent was to enclose an area of mixed vegetation that was characteristic of the dominant meadow features. The radiometers (Figure 6d) were mounted above this surface and the ground sensors were buried within it and the area was left undisturbed throughout the measurement period. The ground sensors measured heat flux, soil temperature and volumetric water content were buried beneath the soil at various depths within the enclosed area (Figure 6e).

The sonic anemometer (Figure 6b) and high frequency gas analyzer (Figure 6c) were mounted at a height of 2.44 m with a horizontal separation of about 10 cm in order to have a strong level of confidence that the instruments were simultaneously sampling the same eddies (Burba 2013). The instruments were oriented to the north so that the dominant turbulent patterns coming from westerly and easterly dominant directions were sampled without obstruction from the tower and other instrumentation. This configuration and instrumentation is consistent with similar eddy covariance studies conducted within mountain meadows (Kato et al. 2004; Dong et al. 2011; Maher et al. 2015).

3.3 Data Processing, Rejection and Uncertainty

Due to high variability and random error associated with making high frequency micrometeorological measurements across the surface-atmosphere interface, quality control standards were applied to the EC data in order to generate defensible and representative measurements. These criteria were applied during post-processing. Data that meets the following quality control standards were used for analysis in this experiment.

3.3.1 Plausible Limit Testing

Random errors generated by the tumultuous physical environment or isolated instrument error can cause a measurement to exceed values that are reasonable (Goulden et al. 1996; Papale et al. 2006). Since spikes and noise can affect between 0 and 15% of

flux measurements (Burba 2013), data were rejected if they fell outside a range of acceptable values. Spikes in the high frequency data were removed before the half-hourly covariances were calculated. In addition, the flux calculations were subject to plausible limit testing during post-processing. For example, CO₂ flux values that were less than -2 and more than 1 mg C m⁻² s⁻¹ were considered implausible after examination of the complete record and rejected during post-processing.

3.3.2 Insufficient Turbulence

EC measurements require a minimum level of turbulence in order to accurately resolve the turbulent exchanges between the surface and the atmosphere (Massman and Lee 2002; Papale et al. 2006; Burba 2013). Low turbulence results in an underestimation of the flux data. In general, the quality of flux data declines as friction velocity decreases and results in an underestimation of the flux (Massman and Lee 2002; Papale et al. 2006). The friction velocity (u^*) threshold for rejection varies based on the ecosystem being sampled and typically ranges between <.05 and 0.2 m/s (Massman and Lee 2002). Papale et al. (2006) suggested a method to determine site-specific appropriate threshold for data rejection. Using this method, the threshold for this site was established at $u^*>=0.1$ m/s, below which data were rejected. Data rejection based on low friction velocity shows a strong bias toward the nighttime hours because nocturnal stability suppresses convective mixing.

3.3.3 Footprint Assessment

The flux footprint, or fetch, is a term used to describe the source area of the measurements being taken by the EC instruments (Papale et al. 2006; Aubinet et al. 2012). An analytical flux source area model developed by Hsieh et al. (2000) was applied to this experiment in order to estimate the flux footprint for each 30-minute block average. The flux footprint model incorporates Lagrangian stochastic dispersion models and dimensional analysis to relate atmospheric stability, measurement height and surface roughness length in order to produce valid estimates of the source area (Hsieh et al. 2000). Field testing of this model showed that the measurement height-to-fetch ratios varied most significantly as a function of atmospheric stability with 1:100 m (unstable), 1:250 m (neutral), and 1:300 m (stable) (Hsieh et al. 2000). This means that measurement height and tower location within the study area should operate within these ranges and take into consideration the relative atmospheric stability and surface roughness of the target ecosystem.

Loney Meadow provides a challenge for EC measurements due to its relatively small size, requiring close inspection of the source area of measurement for each 30-minute period. The meadow boundary was defined from analysis of satellite imagery (Figure 1) and the radial distance from the tower to the meadow boundary was evaluated for 21 directions. Based on the actual observations for each 30-minute averaging period, the analytical footprint model of Hsieh et al. (2000) was used to simulate the source area.

Data were established as high quality if 90% or more of the source area fell within the meadow boundary. A more relaxed second level of data was established when more than 70 percent of the source area was within the meadow boundary.

3.4 Partitioning and Gap Filling CO₂ Exchanges

Rejection criteria and/or instrument error generate gaps in the observed data stream. In order to preserve continuity and generate defensible estimates of the CO₂ flux at various temporal scales, there are a number of commonly used approaches to gap fill EC data (Baldocchi 2003; Falge et al. 2001). For example, regression models, empirically derived algorithms and/or averaging can be applied to fill a gap (Baldocchi 2003). These strategies are generally based on environmental drivers like soil temperature and photosynthetically active radiation (PAR) that show an empirical relationship to carbon fluxes (Crawford et al. 2011).

By measuring the flux of CO₂ between surface and the atmosphere, the EC instrumentation directly measures net ecosystem exchange (NEE), which is derived as the balance between gross primary production (GPP) and heterotrophic plus autotrophic respiration (RE) illustrated by this equation:

$$\text{NEE} = \text{RE} - \text{GPP} \quad (2)$$

For this study, a negative (-) sign convention was given to NEE values that indicate a net uptake of CO₂ from the atmosphere (sink) and positive (+) values are attributed to a net

release of CO₂ to the atmosphere (source). Partitioning the observed NEE data into its two components is a common practice in eddy covariance research (Wohlfahrt et al. 2005; Stoy et al. 2006; Aubinet et al. 2012).

Previous studies have shown that soil temperature has a strong correlation with respiration (Xu & Baldocchi 2004; Gilmanov et al. 2005; Wohlfahrt et al. 2005). With no solar radiation to drive GPP at night, we assumed that all nighttime CO₂ fluxes were entirely composed of respiration and proceeded to model daytime respiration based on its relationship to the observed soil temperature (Wohlfahrt et al. 2005; Moffat et al. 2007). This relation was found to be linear in nature and nighttime CO₂ fluxes were used to generate a linear model for respiration based on the bin averaged soil temperature (T_s).

Observed good quality values of nighttime NEE were identified as observed RE and daytime/missing RE were estimated using the model shown above. In order to account for the impact on respiration due to other environmental controls such as soil moisture and the changes in phenology and biomass of the meadow vegetation, throughout the growing season, the soil temperature-respiration relationship was applied to four distinct seasonal periods, identified from the initial analysis of the NEE observational record. Details of these are provided at the outset of the results section. The model was then used to gap-fill periods when RE was missing (during all daylight hours) and to replace data rejected using the criteria outlined in Section 3.3.

For all daylight hours, GPP values were calculated by residual using Eq. 3 so that

$$GPP = NEE + RE \quad (3)$$

GPP during nocturnal hours was assumed to be 0. Gaps in GPP data during daylight hours were filled using light response models. Light use efficiency (LUE) represents the ratio of PAR to photosynthetic uptake of CO₂ (GPP). Based on similar studies, this relationship was used to fill gaps in GPP by applying a rectangular hyperbola model for all accepted daylight GPP estimates at the 30-minute timescale (e.g. Xu and Baldocchi 2004; Gilmanov et al. 2007; Oliphant et al. 2011).

$$GPP = \frac{\alpha \times A_{max} \times PAR}{A_{max} + \alpha \times PAR} \quad (4)$$

Alpha (α) represents the initial slope of the LUE curve and A_{max} is the point of maximum carbon assimilation. Since the relationship between PAR and photosynthesis is expected to change based on seasonal patterns of vegetation density, the LUE modeling approach is applied to the four distinct phases of the growing season identified.

3.5 Accuracy Assessment: Energy Balance Closure

It is widely held that eddy covariance has as a tendency to underestimate convective fluxes, though the exact mechanisms responsible, and therefore corrections to apply are not well agreed upon (e.g. Stoy et al. 2013). Some underestimation is expected due to unmeasured turbulent transport at higher frequencies than the 10 Hz sampling is able to resolve and longer than 30-minutes, which is the averaging frequency in this case (Wilson et al. 2002). Although this finding is consistent over almost all ecosystems

examined, the underestimation tends to be larger for measurements made in complex or heterogeneous terrain due to the role of advection, particularly from local-mesoscale circulations (Stoy et al. 2013; Foken et al. 2011).

Assuming the surface energy balance (SEB) is balanced and because all principle components of the SEB are frequently measured by EC systems, energy balance closure itself can be used to test the quality of the flux measurements and to diagnose problems (Baldocchi 2008). The simple SEB equation can be rearranged to separate the EC-derived sensible and latent heat fluxes (Q_H and Q_E respectively) from the radiative (Q_N) and storage fluxes (ΔQ_S),

$$\frac{Q_H + Q_E}{Q_N - \Delta Q_S} = 1 \quad (5)$$

Net radiation (Q_N) was derived from the sum of the four component radiative measurements consisting of incoming shortwave (K_{dn}), reflected shortwave (K_{up}), incoming longwave (L_{dn}) and surface emitted longwave (L_{up}) radiation. ΔQ_S was calculated using the average of the two ground heat flux plates plus the estimated soil heat storage in the soil column above the heat flux plates derived from Oke (1987).

For all accepted 30-minute periods when all four components of Eq. 5 were measured, the linear relationship was found by regression between the sum of the turbulent fluxes ($Q_H + Q_E$) and the available energy ($Q_N - \Delta Q_S$). Ideal SEB closure would therefore be reflected by a 1:1 relationship or a solution of Eq. 5 of 1 (Stoy et al. 2013).

Typically, EC studies show a shortfall of 10 – 40% and while good closure does not mean the measurements are definitely valid, poor closure definitely indicates a problem with the measurements (Balocchi 2008; Burba 2013).

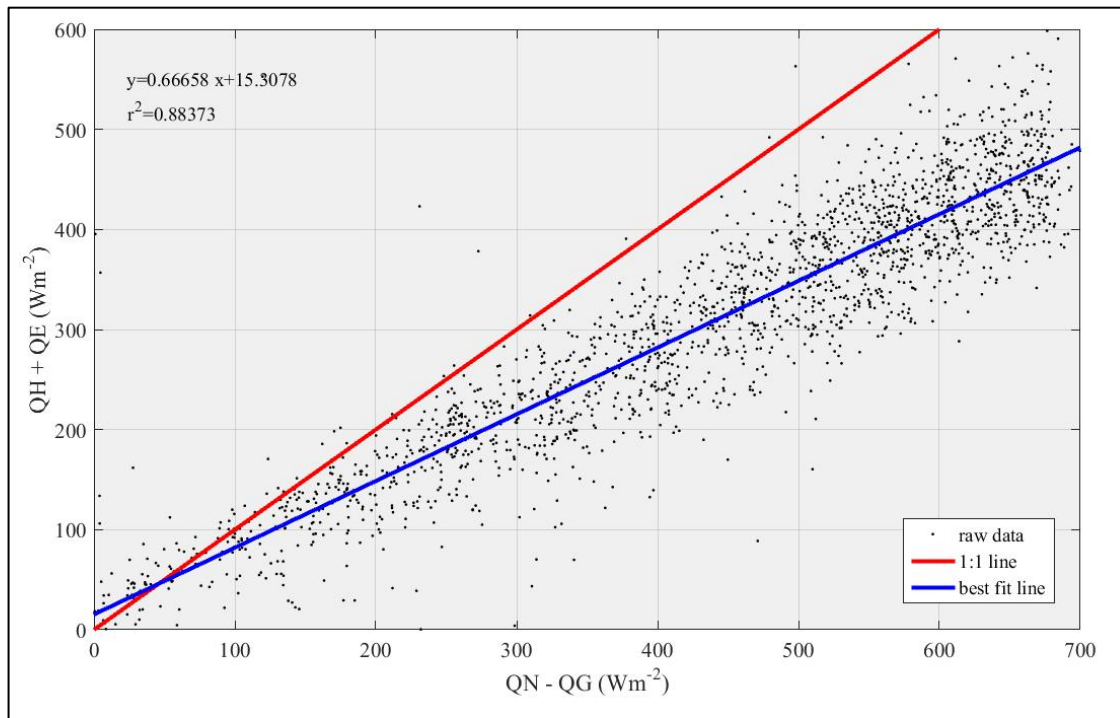


Figure 7. Energy balance closure for all good data with turbulent fluxes on the y-axis and available energy on the x-axis.

Analysis of energy balance closure for the Loney Meadow dataset from this study showed that the slope of the relation is about 0.67. This indicates that closure is about 67%, which means that about 33% of the energy is potentially missing from the flux measurements (Figure 7). The R^2 value indicates that about 88% of the variance in turbulence fluxes can be explained by the regression (Figure 4). The slope of 0.67 is a little lower than the average but well within the distribution of closure estimates from

synthesis studies comparing multiple sites (e.g. Wilson et al. 2002, Stoy et al. 2013). In particular, these values are similar to other studies in complex settings (Stoy et al. 2013), including other meadows in the Sierra Nevada (Castelvi and Oliphant 2017).

Energy balance closure was also used to test the quality of the measurements under different rejection criteria outlined above as well as differences between seasonal periods (Table 3). The slope decreases from 0.67 (All Good Data) to 0.6 for the emergence phase (Period 1) and improves slightly to 0.69 during the two senescence phases (Periods 3 & 4) but, overall, seasonality has little effect on the quality of the measurements. Relaxing the fetch status rejection criteria had no significant effect on energy balance closure suggesting that good data were not severely limited by measurements coming from outside the meadow boundary. Closure was also tested for different levels of friction velocities. The slope of the line drops significantly when the u^* threshold is below 0.1 m/s, which reduces the overall confidence in measurements associated with low friction velocity (Table 3). The lack of significant weakening of SEB closure between difference between a u^* threshold of 0.1 and 0.2 m/s confirms the independent method of Papale et al. (2006) that we used to determine the site specific u^* threshold.

Table 3. Energy balance closure statistics using linear regression after applying testing criteria to flux data.

Testing Criteria	Slope	Y-Intercept	R²	n
Period 1	0.6	16.2	0.75	330
Period 2	0.65	18.6	0.9	637
Period 3	0.69	9.7	0.93	688
Period 4	0.69	14.1	0.91	514
$u^* < 0.1 \text{ m/s}$	0.43	11.2	0.48	2022
$u^* \geq 0.1 \text{ & } u^* < 0.2 \text{ m/s}$	0.61	15.1	0.83	862
$u^* \geq 0.2 \text{ m/s}$	0.67	15.3	0.88	2184
Relaxed Fetch Status	0.66	14.6	0.9	3042
All Good Data	0.67	15.3	0.88	2184

4.0 RESULTS

4.1 Observed Net Ecosystem Exchange of CO₂

As described in Section 3.4, NEE was directly measured by the EC instruments and partitioned into its component fluxes, GPP and RE, during post-processing using empirical models. EC measurements are continuous, which provides the opportunity to examine the CO₂ exchange at various temporal scales. This section describes the pattern and magnitude of NEE at the daily time scale using diurnal ensemble averages and at the seasonal scale using daily total NEE values observed throughout the study period.

4.1.1 Diurnal Patterns of Net Ecosystem Exchange

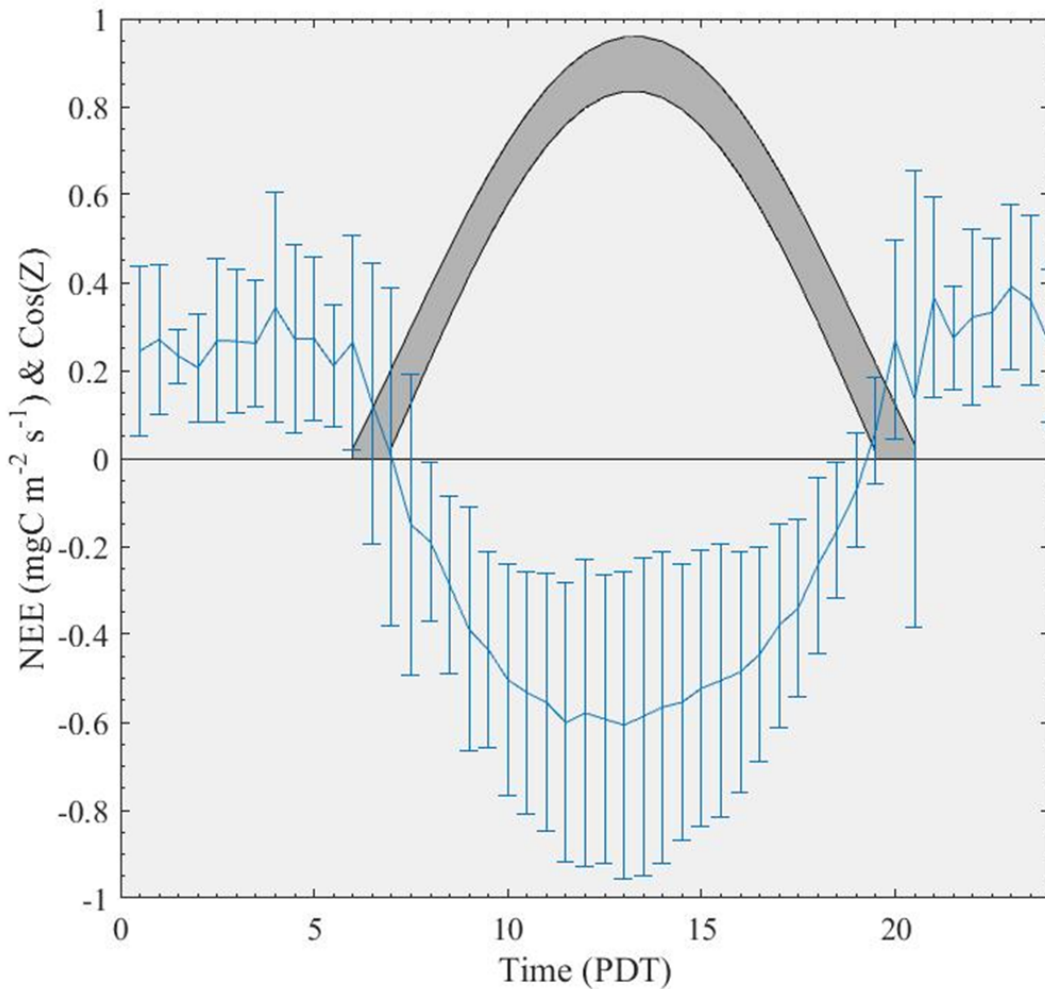


Figure 8. Diurnal 30-minute ensemble averages of NEE at Loney Meadow with error bars representing +/- one standard deviation for the entire observation period. The shaded arc represents the cosine of the solar zenith angle (Z) for minimum and maximum solar declination during the observation period.

Based on ensemble averages over the course of the study period, Figure 8 shows that the ecosystem was a strong net sink of CO₂ from the atmosphere during the day and

a weak source during the night. The shift from source to sink occurred at about 7:00 PDT and returned to a source at about 19:00 PDT, closely associated with astronomical sunrise and sunset times. NEE remained fairly consistent at night, suggesting relatively little change in respiration rates over the diurnal cycle, while the strong daytime signal appears to respond closely to light available to drive photosynthesis. The pattern of NEE exhibits a symmetrical diurnal cycle with peak uptake occurring at about 12:00 PDT. The variability of NEE, demonstrated by the error bars, is greater during the day suggesting more day-to-day variability in photosynthesis than respiration. There is also more variability during the sunrise and sunset hours, which is likely attributed to changes in day length as the growing season progressed (Figure 8). The solar zenith angle (Z) is the ratio of incoming solar radiation at 0° compared to the amount arriving at an angle. This arc is used as a proxy for potential solar radiation, which almost exactly mirrors the pattern of daily NEE. This shows that NEE is closely associated with the solar cycle and that light drives the daily uptake processes in the meadow with little difference between morning and afternoon hours.

On average, NEE peaked at about $-0.6 \text{ mgC m}^{-2} \text{ s}^{-1}$ in the middle of the day when light levels were close to maximum. The mean nocturnal respiration flux shows more consistency ranging between 0.2 and $0.4 \text{ mgC m}^{-2} \text{ s}^{-1}$ (Figure 8). The average daily total net ecosystem exchange for the entire observed study period was $-7.71 \text{ gC m}^{-2} \text{ d}^{-1}$, which changed significantly as the growing season progressed.

4.1.2 Seasonal Patterns of CO₂ Exchanges

Seasonality was a major control on the CO₂ exchange in the meadow over the course of the study period. Based on visual observations of the pattern of NEE shown in Figure 9, the study period was divided into distinct growth periods that describe the seasonal patterns with details provided in Table 4. NEE fluctuated significantly throughout the 2016 growing season with the meadow acting as a net sink of CO₂ for 82 of the 112 days measured. The range of NEE showed a peak uptake of -18.51 gC m⁻² d⁻¹ during the middle of the growing season and a peak source of 2.97 gC m⁻² d⁻¹ occurring near the end of the observation period when senescence of meadow vegetation was clearly visible (Figure 9).

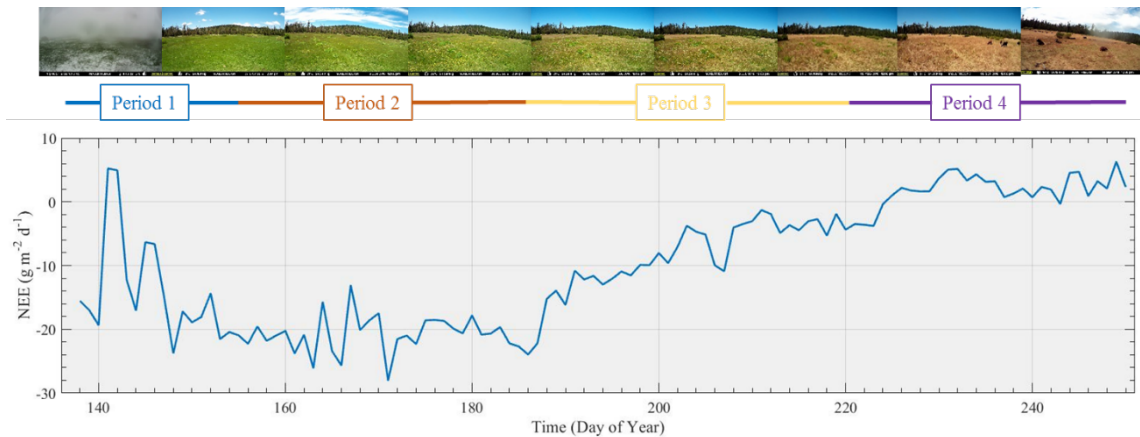


Figure 9. Daily total NEE for the entire study period (bottom). Selected images of meadow surface (west facing) taken from the top of flux tower and approximation of distinct phases of the growing season divided into four periods (top).

The magnitude and sign of NEE varied based on the phase of the growing season as well as on an episodic basis (day-to-day variability) within seasonal phases. The initial trend of NEE decreased from about Day 138 (April 25) to Day 157 (May 16). During this period (Period 1), vegetation rapidly emerged over a very wet surface following snowmelt in the meadow. With the entire meadow covered in snow just 22 days before the study began, this shows a very rapid shift to near peak CO₂ uptake. Period 2 was identified when the NEE signal reached its peak uptake and remained fairly constant until about Day 187 (July 5), with daily total fluxes ranging between -20 and -25 g CO₂ m⁻² d⁻¹. The peak value for daily total NEE during this period was observed at -28 gC m⁻² on Day 171 (June 19). This period was also characterized by maximum vegetation height and density. Following this, began a long and steady rise in NEE, which continued to the end of the study period. This long period was broken into two, Period 3 (early senescence) and Period 4 (late senescence) with the division being the approximate date that the meadow ecosystem switched from the sink to a source on a daily basis (Day 224, August 11). The main environmental characteristics of each of the four phases of the growing season identified are provided in Table 4. These seasonal periods were used separately for driving CO₂ partitioning and gap-filling models as described in Section 3.4 and the results are presented in the following section.

Table 4. Growing season phases identified with date ranges, descriptions, images of the meadow surface and environmental conditions.

	Period 1 (May 17 – Jun 5)	Period 2 (Jun 6 – Jul 5)	Period 3 (Jul 6 – Aug 7)	Period 4 (Aug 8 – Sep 6)
Description	Vegetation emerged, NEE decreased	Peak growth, NEE plateaued	Beginning senescence, NEE increased	Most vegetation senesced, NEE became positive
Average PAR ($\mu\text{mol m}^{-2} \text{s}^{-1}$)	633	764	782	656
Average Soil Moisture (%)	53	47	23	10
Total Precip. (mm)	34	0.5	0	0.5
Average Daily Air Temp. (°C)	Max: 16.2 Mean: 9.6 Min: 1.7	Max: 20.4 Mean: 13 Min: 3.4	Max: 23.4 Mean: 14.5 Min: 3.6	Max: 23.5 Mean: 14 Min: 3.7
Image				

4.2 CO₂ Flux Partitioning into RE and GPP

Partitioning of the CO₂ flux and gap-filling was conducted in the manner described in Section 3.4. Here, the site and seasonal period-specific model coefficients and statistics are presented and the implications for biophysical controls on the CO₂ flux are discussed.

4.2.1 Ecosystem Respiration

Both heterotrophic and autotrophic respiration show a strong correlation to soil temperature and soil moisture (Flanagan et al. 2002). The nocturnal CO₂ flux was assumed to be entirely comprised of respiration. Similar to previous studies, nighttime CO₂ flux data was used to model daytime RE values based on the relationship between the isolated nocturnal CO₂ flux and soil temperature (Schmid et al. 2000; Xu and Baldocchi 2004; Gilmanov et al. 2005; Wohlfahrt et al. 2005). Figure 10 shows the model using the binned averages in 1°C increments for the entire study period. The trend is positive and linear and, with an R² of 0.95, the relationship appears to be strong. The relationship using the raw data (non-binned data) shows a much higher degree of scatter and a significantly weaker relationship (R²=0.09). The low R² value of the raw data indicates that, while soil temperature is a general biological control on RE, other factors are driving the variability at the 30-minute timescale. These factors may include wind speed associated with turbulent exchange rates, variation in the source area based on wind direction, the presence or absence of cattle on the meadow and other forces that might affect the measurements at the 30-minute time scale. Because of significant changes in leaf phenology and soil moisture over the course of the growing season (Xu and Baldocchi 2004), the respiration model, using binned averages, was applied to each of the growth periods and the resulting statistical parameters are presented in Table 5.

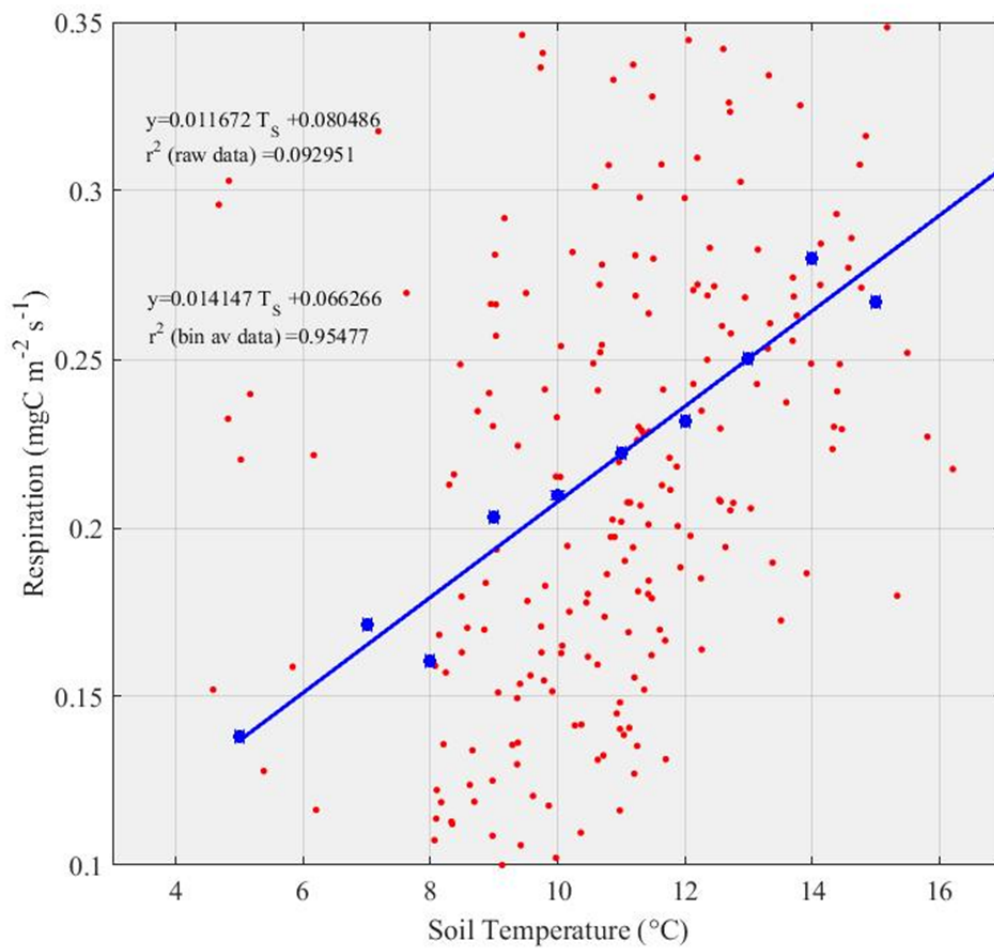


Figure 10. Soil temperature response of nocturnal respiration with binned average temperature in 1°C increments.

Table 5. Regression parameters and statistics for respiration model using binned averages and divided into seasonal periods (1–4) and the entire study period (ALL) with average observed nighttime RE.

Seasonal Period	Slope	Y-Intercept	R ²	n	Average Nighttime RE (mgC m ⁻² s ⁻¹)
ALL	0.0141	0.0521	0.95	248	0.206
1	0.0114	0.0678	0.27	47	0.177
2	0.0134	0.0663	0.85	95	0.216
3	0.014	0.0678	0.62	71	0.228
4	0.0194	0.086	0.42	28	0.155

Period 2 shows the strongest relationship between nocturnal respiration and soil temperature, while Period 1 exhibits the weakest relationship. A snow event occurred during the first period, which may explain some of the disparity between the R² values of Period 1 compared to Periods 2 and 3. The snow may have sealed the soil from the atmosphere and saturated the surface as it melts, which could reduce soil respiration initially when oxygen is less available in the soil and may increase it due to moistening of surface soil following melt. In addition, this period exhibits the largest variation in plant density, which may contribute to the variability of the relationship. The lower R² values in Periods 1 and 4 could also be explained by the lower sample size compared to Periods 2 and 3.

The model coefficients generated by the linear regression are quite similar for the four seasonal periods and total soil respiration does not change significantly over the course of the study period. Average nighttime RE, in terms of magnitude followed a similar seasonal pattern to NEE, which peaked in Period 2 and reduced as the vegetation senesced. This indicates that autotrophic respiration by plants is a significant component of ecosystem respiration in the meadow throughout the season. The relatively small slope of the model (Table 5) indicates that soil temperature explains some dependence for RE, but not as significantly compared to previous studies (e.g. Flanagan et al. (2002) =0.164).

4.2.2 GPP and Light Use Efficiency

Photosynthesis is driven by the amount of available photosynthetically active radiation (PAR). The light response of GPP was determined by applying a rectangular hyperbola function (Eq. 5) to each seasonal period (Figure 11) (Gilmanov et al. 2007; Olyphant et al. 2011). The high α value for Periods 1 and 2 indicate a strong response to light until the vegetation begins to senesce during the late summer and fall months. The point of maximum CO₂ assimilation (A_{max}) varied significantly throughout the season (47 < A_{max} < 247 $\mu\text{mol m}^{-2} \text{s}^{-1}$) (Table 6). A comparison study of twenty European grasslands by Gilmanov et al. (2007) reported α values with a minimum of 0.016, a maximum of 0.075, a mean of 0.048 $\mu\text{mol mol}^{-1}$, and a similar range in A_{max} values (mean ~42.5 < A_{max} < 216 $\mu\text{mol m}^{-2} \text{s}^{-1}$). With a total study period α of 0.0741, the light response

observed in Loney Meadow was most similar to the wetter grasslands surveyed by Gilmanov et al. (2007).

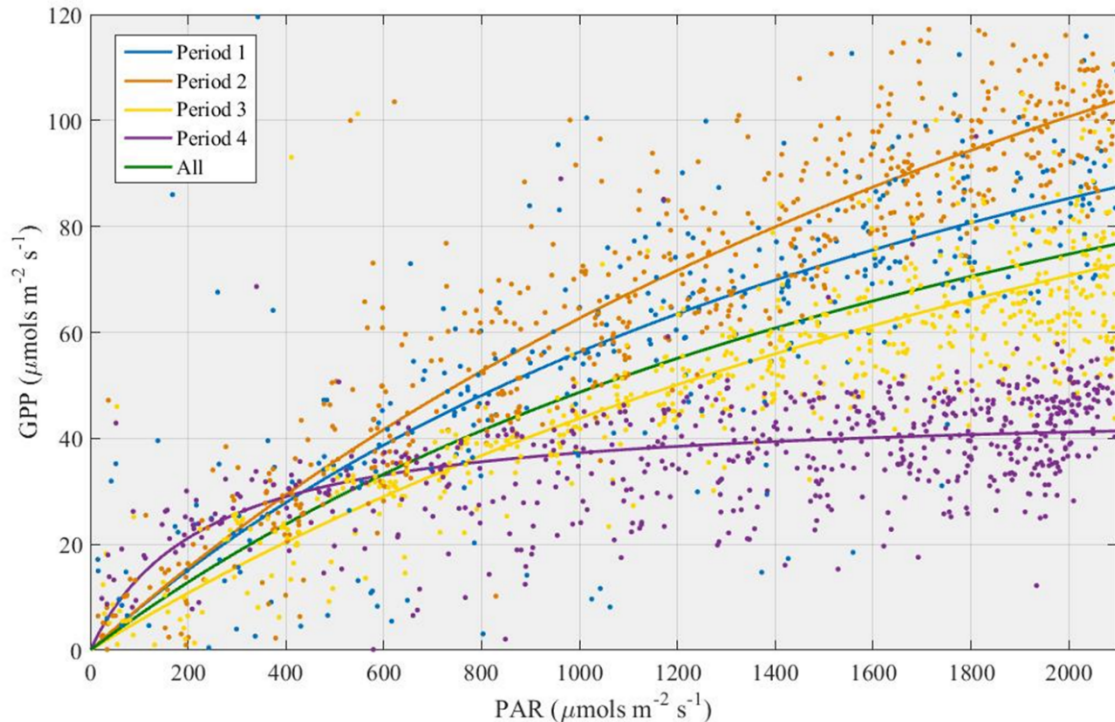


Figure 11. LUE curves for the total study period and separated into four seasonal periods.

Table 6. LUE curve parameters and statistics with average observed GPP.

Seasonal Period	α	A_{\max}	R^2	n	Average GPP ($\text{mgC m}^{-2} \text{s}^{-1}$)
ALL	0.0741	154.3	0.41	2548	0.704
1	0.0849	173.7	0.57	411	0.774
2	0.0861	246.7	0.82	718	0.91
3	0.0609	172.9	0.67	766	0.685
4	0.223	47	0.08	637	0.454

With an R^2 value of 0.82, data from Period 2 is most closely fitted to the regression curve and shows the strongest response to light compared to the other three seasonal periods. With a very low level of light saturation (about $800 \mu\text{mol m}^{-2} \text{s}^{-1}$) and a low R^2 value (0.08), Period 4 shows the weakest relationship between GPP and PAR signaling that photosynthesis is suppressed by senescence resulting in a mostly flat LUE curve. When PAR reaches $2000 \mu\text{mol m}^{-2} \text{s}^{-1}$, GPP during Period 4 is about a third of what is observed during Period 2 (Figure 11). The overall leaf density during Period 4 did not change significantly; however, the amount of green leaves has massively reduced at this point in the season. The flattened curve and low R^2 value during this period of senescence suggest that the relationship between PAR and photosynthesis had almost entirely disconnected.

4.3 Diurnal Controls on Ecosystem CO₂ Exchange

Based on the overall magnitudes reported in Tables 5 and 6, NEE is clearly driven more strongly by GPP than RE. The result is that the diurnal pattern of NEE closely mirrors that of GPP. The diurnal pattern of GPP was mostly symmetrical during all four seasonal periods and showed a similar rate of CO₂ uptake in the morning and decline in the afternoon (Figure 12a). Photosynthesis began between 5:00 and 7:00 PDT and shut down by about 21:00 PDT for all four seasonal periods. The diurnal pattern of Periods 1, 2 and 3 were similar in shape but differed in overall magnitude at the peak. Period 4 GPP had a distinctly different shape than the previous seasonal periods; it mostly flattens at

about 10:00 PDT at a magnitude of about $0.5 \text{ mgC m}^{-2} \text{ s}^{-1}$. With the exception of Period 4, the pattern of GPP is very similar to the daily cycle of PAR (Figure 12a and 12c). Light levels were quite similar throughout all four seasonal periods with the lowest values observed during Period 1 and the highest occurring in Period 3, which coincided with the summer solstice (Jun 20). Despite abundant light available for photosynthesis, Period 3 GPP peaks at about $0.85 \text{ mgC m}^{-2} \text{ s}^{-1}$ compared to $1.26 \text{ mgC m}^{-2} \text{ s}^{-1}$ in Period 2. This is explained by a significant reduction in volumetric water content (VWC) (Figure 12f) and an increase in vapor pressure deficit (VPD) (Figure 12e). With limited water availability and a high atmospheric demand for water, vegetation became stressed and GPP declined despite high levels of light.

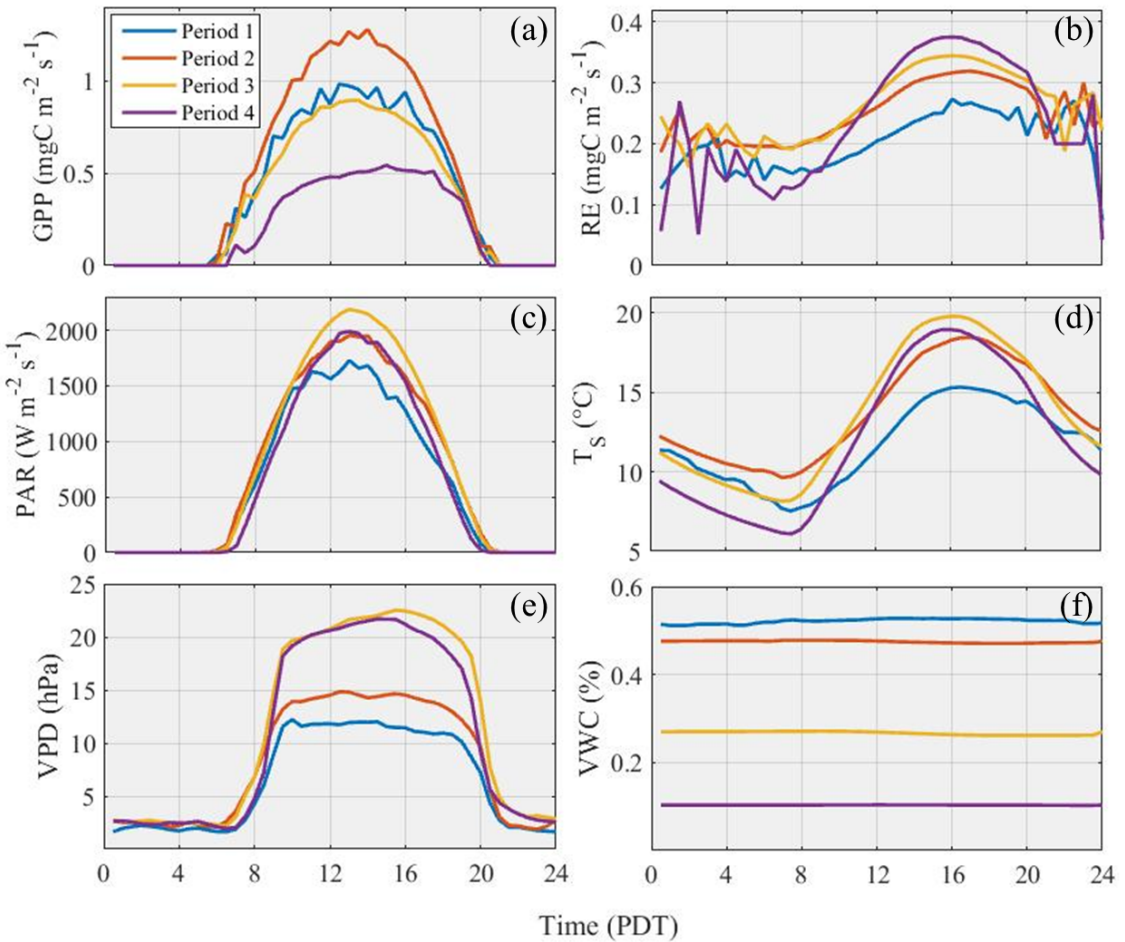


Figure 12. Diurnal ensemble 30-minute averages of GPP (a), RE (b), PAR (c), soil temperature (T_s) (d), vapor pressure deficit (VPD) (e), and volumetric water content (VWC) (f) according seasonal period.

Unlike GPP and NEE, RE exhibits a somewhat asymmetrical diurnal cycle with a gradual incline in the morning, peaking between 15:00 and 17:00 PDT, and declining slightly during the night (Figure 12b). The much less variable daytime pattern relative to nocturnal hours is due to the fact that all daytime values are provided by the empirical model, while accepted nocturnal CO₂ flux data were used for night values. Since many

nocturnal periods were rejected due to insufficient turbulence, these averages are based on relatively small samples. The diurnal asymmetry is explained by the model, which is driven linearly by soil temperature, which peaked in mid-afternoon (Figure 12d). The diurnal range in RE is only about one quarter of GPP. On a seasonal basis, Period 1 exhibited the lowest RE rates. This is likely explained by the lower soil temperature (Figure 12e) and high level of water saturation (Figure 12f), which can have a suppressing effect on root and soil respiration if water pools at the surface because it creates a barrier between the soil and the atmosphere. The average daily total RE rate for the entire study period was $21.24 \text{ gC m}^{-2} \text{ d}^{-1}$ (Table 7). Daily average RE rates for each season were very similar to the mean with the greatest deviation occurring in Period 1 ($17.42 \text{ gC m}^{-2} \text{ d}^{-1}$), which exhibited the lowest overall RE rate for the study period (Figure 12b). However, the peak value of RE consistently increased as the season progressed reaching a maximum emission of about $0.38 \text{ mgC m}^{-2} \text{ s}^{-1}$ during Period 4 (Figure 12b).

Table 7. The average daily CO₂ flux values for each seasonal period and the entire study period.

Seasonal Period (Day of Year)	GPP (gC m⁻² d⁻¹)	RE (gC m⁻² d⁻¹)	NEE (gC m⁻² d⁻¹)
Period 1 (138 – 157) May 17 - June 5	34.05	17.42	-13.65
Period 2 (158 – 187) June 6 - July 5	42.96	21.6	-18.51
Period 3 (188 – 220) July 6 - August 7	31.06	22.51	-5.48
Period 4 (221 – 250) August 8 - September 6	18.78	20.32	2.97
Total Study Period (138 - 250)	31.76	21.24	-7.71

4.4 Seasonal and Synoptic Controls on Ecosystem CO₂ Exchange

The ancillary micrometeorological measurements taken concurrently with the EC measurements provide the opportunity to explore environmental variables and their effect on surface-atmosphere exchanges over the seasonal cycle (Figure 13). As discussed previously, the primary environmental drivers associated with CO₂ exchanges are PAR, temperature and water availability. Regional scale climate trends such as drought and El Nino affect the seasonal pattern of these drivers, which represents a significant control on the variability of CO₂ exchanges from year to year. Synoptic scale changes are associated with dynamic weather conditions like cloud cover and precipitation.

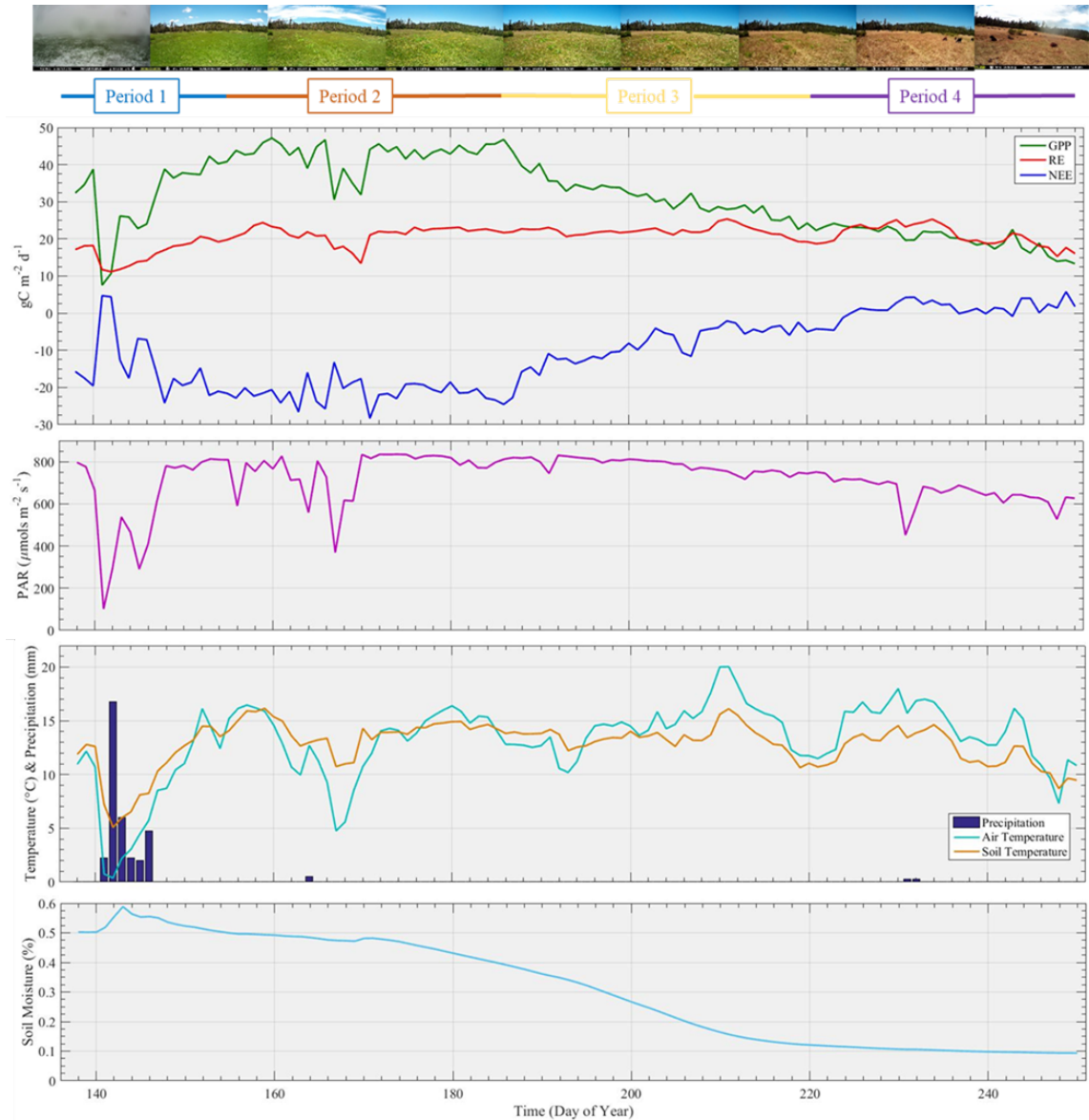


Figure 13. Daily total CO_2 exchanges between the meadow surface and the atmosphere throughout the growing season (a) and (in descending order) environmental controls including daily average photosynthetically active radiation (PAR) (b), air/soil temperature (c), daily total precipitation (c) and soil moisture (d). (Top) Selected images of meadow surface (west facing) taken from the top of flux tower and approximation of distinct phases of the growing season divided into four periods.

The seasonal pattern of GPP closely mirrored that of NEE indicating that it was the driving component of seasonal variability of the CO₂ flux. Because the trend of GPP plateaued between June 5 and July 6, Period 2 represents the time in the growing season that we can assume that leaf area index (LAI) has reached its maximum. Peak values of GPP reached 47 gC m⁻² d⁻¹ during Period 2 and declined to about 14 g CO₂ m⁻² d⁻¹ by the end of the study period (Figure 10). RE showed much less variability than GPP remaining between 17 and 27 gC m⁻² d⁻¹ throughout most of the study period.

A snow event occurred during Period 1 (Day 141) and covered the meadow in snow for about two days. This event generated a significant decrease in GPP from about 40 gC m⁻² d⁻¹ on Day 140 to about 8 gC m⁻² d⁻¹ on Day 141. RE was suppressed but not affected as dramatically as GPP, which caused the ecosystem to shift from a sink of about -20 gC m⁻² d⁻² to a small source (~5 gC m⁻² d⁻¹) for about two days. This weather event also generated the lowest recorded PAR (~100 W μmols m⁻² s⁻¹) and temperature (Air < 1° C & Soil < 6° C) during the observation period (Figure 13b & 13c). After the snow melted, GPP continued to increase until it mostly flattened on June 5, which marked the end of the emergent phase.

Between June 12 and 19 a small storm generating about 1 mm of precipitation affected the CO₂ budget in the meadow. At the onset of the storm on Day 164, PAR decreased to about 560 W μmols m⁻² d⁻¹ and a decrease in GPP (~5 gC m⁻² d⁻¹) was observed with little to no initial effect on RE (Figure 13a & 13b). As the weather event

progressed, average daily temperature declined by about 3° C and PAR reached a minimal level of 375 W $\mu\text{mols m}^{-2} \text{d}^{-1}$ (Day 167). With reduced PAR and temperature, both GPP and RE responded by decreasing sharply and NEE was similarly reduced but, unlike the snow event in Period 1, the ecosystem remained a net sink of CO₂ from the atmosphere. With a smaller decrease in temperature compared to PAR, the precipitation/cloud event had a less significant effect on RE rates compared to GPP (Figure 13a, 13b and 13c). On a daily basis, PAR appears to be the primary driver of the fluctuating pattern of GPP throughout the study period. However, according to the LUE analysis shown in Figure 8, that relationship weakens as the vegetation senesces. This decoupling is evident in Period 4 when a small storm causes PAR to decrease and this event has a much less pronounced effect on the seasonal trend of GPP.

Soil moisture levels declined gradually after the snow event saturated the soil in Period 1 (Figure 13d). Despite maintaining mostly consistent values for PAR, Period 3 represents the phase at which vegetation began to senesce, which is evident by the steady decline in GPP and the daily surfaces images showing a shift in color from green to brown (Figure 13). A sharp decline in soil moisture from about Day 171 appears to be the main driver of this seasonal change that initiated senescence and the onset of Period 3. When soil moisture levels reached about 40%, GPP began its steady decline. This reduction in GPP had little to no effect on RE observed in the meadow. The declining rate of GPP with no change in emission rates caused the magnitudes of NEE to fall similarly to GPP.

On about August 8 (Day 221), the meadow ecosystem switched from a very weak sink of CO₂ to a source. At this point ecosystem respiration had surpassed GPP (Figure 13a). By Period 4, day length also decreased, which caused average daily PAR to decrease by about 100 to 200 $\mu\text{mols m}^{-2} \text{s}^{-1}$. In addition, soil moisture levels declined and flattened at about 10% (Figure 13d). A small rain event (< 1 mm) occurred on August 18 (Day 231), but had little to no impact on recorded soil moisture levels (Figure 13c & 13d). At this point, most of the vegetation had become insensitive to light levels and productivity was constrained by limited water availability. On a seasonal basis, declining soil moisture levels appear to be the main environmental driver that controls the larger seasonal trends as they relate to declining productivity and vegetation senescence.

5.0 DISCUSSION

EC measurements showed that, during most of the growing season, Loney Meadow functioned as a strong sink of CO₂ from the atmosphere. After summing the diurnal ensemble 30-minute averages and multiplying by the number of days, the total NEE for the entire study period was approximately -920 gC m⁻². This would be extremely large as an annual budget compared with other terrestrial ecosystems. However, this value excludes both the first 22 days of the snow-free annual cycle, the period of unmeasured senescence before snowfall and during the winter period under snowpack. It also excludes some minor CO₂ fluxes, such as cow respiration and other carbon

exchanges such as methane (CH_4) emissions. The following sections approximate an annual CO_2 budget estimate for Loney Meadow, compare the CO_2 budgets found there to other ecosystems, identify the unmeasured components of the carbon budget and discuss the impacts of degradation and climate variability.

5.1 Annual CO_2 Budget Estimate

A common application of EC research is to facilitate annual carbon budget estimates for terrestrial ecosystems (Baldocchi 2008). Because the measurement period is representative of 4 out of 12 months in 2016, we need to extrapolate the data collected in this study in order to generate an annual CO_2 budget estimate. The total snow-free period of the growing season was addressed first by establishing pre and post measurement periods, which are labeled Period 0 and Period 5. Period 0 represents the days between when snow melted from the meadow surface and the flux tower was installed, and Period 5 represents the time between when the measurements ceased and snow covered the surface again in the late fall. The starting point of Period 0 was established based on the initial site inspection that took place on April 25, 2016. During this assessment, it was observed that about 75% of the meadow surface was covered in snow and that vegetation was beginning to emerge. Using snow water equivalent (SWE) data from a nearby climate monitoring station (SNOWTEL: Robinson Cow Camp, Elevation: 1975 m), the end of the growing season in Period 5 was estimated to be November 24, 2016 (NRCS 2017). Based on the assumption the trend of emergence and senescence are somewhat consistent

over time, linear regression models were derived from the CO₂ flux data in Periods 1 and 4 (Figure 14) and extrapolate daily total GPP, RE and NEE for each day of the unmeasured snow-free days (Table 8).

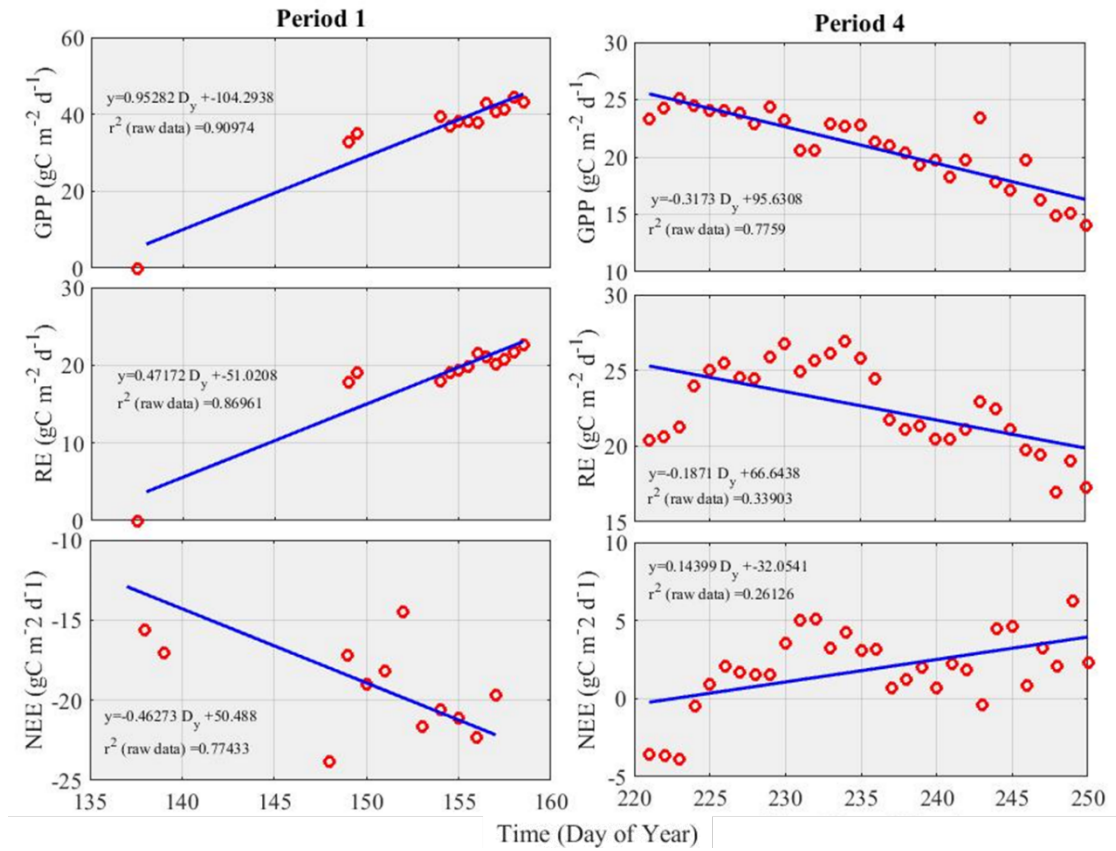


Figure 14. Linear regression of daily total CO₂ flux data for seasonal Periods 1 and 4.

Table 8. Annual CO₂ budget estimates divided into observed seasonal periods (1 – 4), modeled periods (0 and 5) and the estimated flux when snow covered the meadow.

Time (Day of Year)	GPP (gC m ⁻²)	RE (gC m ⁻²)	NEE (gC m ⁻²)
Period 0 (116-137)	352	181	-180
Period 1 (138-157)	681	348	-273
Period 2 (158-187)	1289	432	-555
Period 3 (188-220)	1025	743	-181
Period 4 (221-250)	563	610	89
Period 5 (251-329)	379	838	732
Snow Free Period (116-329)	4288	3152	-367
Snow Covered Period (0-115 & 330-360)	0	145	145
Entire Year (0-360)	4398	3540	-222

When snow covers the meadow surface it shuts down GPP and suppresses respiration. Although significantly reduced, microbes in the soil continue to respire. In a study of five North American grasslands, Svejcar et al. (2008) found an average CO₂ flux during the winter non-growing season of 1.23 gC m⁻² d⁻¹ with a range of 0.68 – 2.11 gC m⁻² d⁻¹. Similarly, Wohlfart et al. (2008) measured a consistent emission rate of 1 g C m⁻² d⁻¹ during the snow covered months of a temperate mountain grassland.

Snow covered the surface of Loney Meadow for approximately 145 days during the 2016 measurement year. Based on the measured snow covered emission rate estimated by Wohlfart et al. (2008), the CO₂ emissions for the 2016 snow covered period was about 145 gC m⁻². If we apply this emission rate to the growing season CO₂ budget for this study site, that puts the estimated total annual CO₂ budget for Loney Meadow in 2016 at -222 gC m⁻² y⁻¹ (Table 8). Given the range in snow-covered estimates in North American grasslands (Svejcar et al. 2008), the range in the annual CO₂ budget is -268 < NEE < -61 gC m⁻² y⁻¹. This indicates that despite applying a comparably large estimation for RE during the snow-covered portion of the study year, Loney Meadow still acted as a net sink of CO₂ from the atmosphere. In addition, there is a degree of uncertainty in the assumptions made by the linear regression method used to extrapolate the unmeasured fluxes of the snow-free period. For example, soil temperature is likely to exhibit a decreasing trend during Period 5, which would have a suppressing effect on RE. With RE somewhat suppressed, this would increase the overall magnitude of NEE and strengthen the sink. CO₂ flux measurements over the full annual cycle in SN mountain meadows are needed in order to improve the annual budget estimations.

5.2 Comparison of Loney Meadow to Wetland and Grassland Ecosystems

The overall pattern of the growing season (Figure 9) shows that the meadow ecosystem functioned as a strong sink of CO₂ during the growth phase and a weak source during the senescence phase. This pattern is similar to previous studies conducted in

grasslands (e.g. Xu and Baldocchi 2004) and wetlands (e.g. Knox et al. 2015) with Mediterranean climates. This pattern is characterized by a steep emergence phase until reaching peak growth (usually in the spring) and a gradual decline in productivity as the vegetation senesces in the summer/fall (Dugas et al. 1999; Flanagan et al. 2002; Xu and Baldocchi 2004; Knox et al. 2015). For example, Xu and Baldocchi (2004) monitored a grassland located at the foothills of the SN (129 m a.s.l.) and found a similar overall pattern of NEE consisting of a strong sink during the growing season and a weak source during the senescence phase. However, the period of net carbon uptake began much earlier in the season and had a longer duration (January – June) compared to this study (Xu and Baldocchi 2004). In addition, peak NEE values (about $-5 \text{ gC m}^{-2} \text{ d}^{-1}$) at the grassland site were much lower than Loney Meadow, which showed a range of -20 to -30 $\text{gC m}^{-2} \text{ d}^{-1}$ during Period 2. In addition, the peak growth phase occurred much later in the growing season compared to the low elevation ecosystems described by Xu and Baldocchi (2004) and Knox et al. (2015). The early spring period of maximum growth observed in many grassland and wetland ecosystems is likely influenced by local climate patterns and low elevations that contribute to warmer overall temperatures with little to no snow falling in the fall/winter. Based on previous research, the complexity of the mountain terrain and the greater water availability generated by the snowpack have a direct effect on the timing and seasonal growth patterns observed in SN meadows (Kattelmann and Embury 1996; Loheide et al. 2009; Lowry et al. 2011; Viers et al. 2013).

The timing of the seasonal growth pattern was more similar to EC studies conducted in meadow ecosystems located in China. A study of a high elevation (3250 m a.s.l.) grazed alpine meadow on the Qinghai-Tibetan plateau showed that the seasonal peak of NEE occurred on July 7, which was slightly later than the peak growth period observed in Loney Meadow (Kato et al. 2004). Dong et al. (2011), observed a similar slightly later peak in a temperate meadow steppe ecosystem. However, the pattern of NEE on a seasonal basis for both of these ecosystems showed a much shorter period of peak growth compared to this study. This indicates that elevation and latitude is likely to be a strong control on the timing of seasonal growth patterns of mountain meadows.

5.2.1 Comparison of Diurnal Patterns and Daily Totals

With an average diurnal peak NEE value of about $-1 \text{ mgC m}^{-2} \text{ s}^{-1}$, Period 2 showed the greatest daily net uptake of CO_2 . Previous studies have shown similar magnitudes of average diurnal NEE during the peak growth period of grassland/prairie ecosystems: $-1.4 \text{ mgC m}^{-2} \text{ s}^{-1}$ (Suyker and Verma 2001), $-1.0 \text{ mgC m}^{-2} \text{ s}^{-1}$ (Ham & Knapp 1998), $-1.2 \text{ mgC m}^{-2} \text{ s}^{-1}$ (Dugas et al. 1999). Despite being on the lower end of the range in terms of peak diurnal NEE, Loney Meadow, in general, showed comparatively high peak daily total NEE values than both wetland and grassland ecosystems. For example, the highest recorded daily CO_2 exchange in a young wetland studied by Knox et al. (2015) was about $-11 \text{ gC m}^{-2} \text{ d}^{-1}$ and a survey of wetlands by Lund et al. (2010) showed maximum daily total NEE values ranging between -1 and $-4 \text{ gC m}^{-2} \text{ d}^{-1}$. Grasslands

exhibit a high degree of variability in peak daily total CO₂ values ranging between -5 (Flanagan et al. 2002; Xu and Baldocchi 2004) and -50 gC m⁻² d⁻¹ (Dugas et al. 1999). Peak values in grasslands that reach values exceeding -20 gC m⁻² d⁻¹, like the sorghum dominated grassland surveyed by Dugas et al. (1999), are rare and generally short lived. Peak values of daily total NEE in Loney Meadow ranged between -20 and -30 gC m⁻² d⁻¹ and produced a high overall seasonal average of -18.51 gC m⁻² d⁻¹ during the peak growth period.

Despite having a somewhat similar seasonal pattern, the daily magnitudes reported in this study were quite different than other meadows surveyed using the EC method. Kato et al. (2004) reported a seasonal peak diurnal CO₂ flux of -0.13 mgC m⁻² s⁻¹ in an alpine meadow (3250 a.s.l.). Similarly, a meadow steppe ecosystem in northeast China showed a large diurnal flux of CO₂ (-0.16 mgC m⁻² s⁻¹) during a wet year (Dong et al. 2011). This exceeds the recorded peak of NEE in Loney Meadow (~1 mgC m⁻² s⁻¹) during Period 2. However, the daily maximum NEE recorded in these two meadow ecosystems in China ranged between -3.9 (Kato et al. 2004) and -6.3 mgC m⁻² d⁻¹ (Dong et al. 2011), which was significantly less than the average daily total NEE recorded in Loney Meadow (-18.51 gC m⁻² d⁻¹). This supports the assessment that mountain meadow ecosystems are highly complex and show a great deal of variability compared to other ecosystems and meadow classifications. Factors that may contribute to this variability are plant community, elevation, latitude, and water availability/distribution across the meadow surface.

5.2.2 Annual Comparison

A synthesis study of wetland ecosystems consisting of peatlands and tundra by Lund et al. (2010) reported average annual net CO₂ uptake of -103 ± 103 gC m⁻² y⁻¹. Two sites in this study showed similar annual NEE values of about -200 gC m⁻² y⁻¹ (Lund et al. 2010). Both of these sites were fen type wetlands with comparably high summertime LAI consisting of vascular plant communities (Lund et al. 2010). Despite having a similar seasonal pattern of NEE and reaching large magnitudes of CO₂ uptake, most grasslands sequester significantly less CO₂ from the atmosphere annually compared to this study (Table 9). Grasslands have been widely studied using the EC method and water availability is consistently identified as a driving environmental control on NEE (Flanagan et al. 2002; Wohlfahrt et al. 2008; Scott et al. 2010). In many cases, drought conditions cause the ecosystem to function as a net source of CO₂ to the atmosphere (Scott et al. 2010; Dong et al. 2011). It is not well understood whether mountain meadows exhibit a similar potential to switch to a net source of CO₂ to the atmosphere on an annual basis.

Table 9. Comparison of Loney Meadow's estimated net annual CO₂ exchange to wetland and grassland ecosystems.

Site Name	Ecosystem Type	Climate Patterns	Elevation (m)	Annual NEE (gC m⁻² y⁻¹)	Citation
San Joaquin Delta, CA	Restored wetland (mature)	Mediterranean Precipitation: 278 mm	-9	-397	Knox et al. 2015
PL-WET	Rich fen (wetland)	Temperate	54	-220	Lund et al. 2010
CA-WP1	Treed fen (wetland)	Boreal	540	-220	Lund et al. 2010
Loney Meadow	Mountain meadow - semiwetland	Mediterranean Precipitation: 51 mm	1822	-222	This study
Tonzi Ranch, CA	Oak/grass savanna	Mediterranean Precipitation: 562 mm	177	Max: -155 Min: -56	Ma et al. 2007
Songnen Plain - Northeast China	Meadow steppe (grassland)	Semi-arid continental monsoon Precipitation: 384 mm (wet)	171	-160	Dong et al. 2011
Songnen Plain - Northeast China	Meadow steppe (grassland)	Semi-arid continental monsoon Precipitation: 207 mm (dry)	171	-64	Dong et al. 2011
Kendall Grassland, AZ	Semidesert grassland/	Arid steppe: N. American monsoon Precipitation: 312 mm	1530	2005: 21 2007: -69 2008: -98	Scott et al. 2010
Vaira Ranch, CA	Open grassland	Mediterranean Precipitation: 562.1 mm	129	Max: -88 Min: 141	Ma et al. 2008

Over the 2016 annual cycle, the CO₂ exchange in Loney Meadow behaved more similarly to wetlands compared to grasslands (Table 9). The net CO₂ flux observed in this study was more than double what was measured during an above average precipitation year (2008) in Kendall, AZ. Yearly precipitation totals that impacted this study were slightly less than average and followed a multi-year severe drought (Table 2). Similar to the study by Dong et al. (2011), we would expect that the annual CO₂ budget would vary significantly with the timing and magnitude of precipitation patterns (Table 9). While the specific impacts of the drought on this study are unclear, the previously mentioned studies suggest that drought reduces the overall magnitude of the CO₂ sink on an annual basis. Despite any potential over or underestimation of NEE associated with extrapolating the unmeasured snow-free period and the RE rate during the snow-covered period, it is clear that Loney Meadow acted as a net sink of CO₂ from the atmosphere in the year 2016. More research that incorporates long-term monitoring is necessary to describe the interannual variability of the SN mountain meadow CO₂ exchange.

5.3 Unmeasured Carbon Fluxes in Loney Meadow

The research presented in this paper focuses on the exchanges of CO₂ between the surface and the atmosphere at the diurnal and seasonal scales. It does not specifically measure other elements of the carbon budget within the meadow ecosystem. The methane (CH₄) flux was not measured. The net flux of dissolved carbon moving through the meadow via the stream network was not measured. Lastly, consumption and emission of

carbon by grazing animals was not specifically monitored. All of these components are a factor when evaluating the entire carbon budget of the ecosystem.

5.3.1 Methane Flux

Similar to low elevation wetlands, wet mountain meadows experience high rates of plant productivity and contain a high density of soil carbon (Norton et al. 2011; Blankinship et al. 2014). In addition, microbial decomposition rates are suppressed during the cold fall/winter months because of the snowpack. This means that mountain meadows have the potential to both store a significant amount of carbon in the soil/biomass as well as emit high levels of CH₄ depending on environmental conditions (Norton et al. 2011).

A study by Blankinship et al. (2014) used a chamber technique to assess the spatial distribution of the CH₄ flux of a SN subalpine meadow (2860 m a.s.l.) during the peak growth (July) and senesced (September) phases of the seasonal cycle. This study found that, of the 48 plots sampled in July, 3 resulted in a net emission; and, of the 24 plots surveyed in September, 1 plot showed a net emission of CH₄ (Blankinship et al. 2014). Overall, there was net uptake of CH₄ from the atmosphere with drier soils consuming about five times more CH₄ than wetter soils (Blankinship et al. 2014). They reported that the CH₄ flux was about -31.3 µgC m⁻² h⁻¹ in the early growth season and -22.6 -31.3 µgC m⁻² h⁻¹ in late growth season (Blankinship et al. 2014). This indicates that, unlike the CO₂ flux, there is a negative relationship between CH₄ emission and soil

moisture. The chamber method used by Blankinship et al. (2014) did not measure seasonal pulses of CH₄ during thawing periods or other synoptic environmental controls that will likely have influenced the net annual CH₄ flux. Since CH₄ uptake was higher under drier conditions, it is important to recognize that SN meadows will exhibit highly variable spatial and temporal trends in CH₄ emission/sequestration, depending most significantly on water availability. More research that includes a stronger temporal dataset is necessary to evaluate seasonal patterns of the CH₄ flux in meadows.

5.3.2 Transport of Dissolved Organic Carbon through Stream Network

Previous studies have shown that small amounts of organic carbon stored in wetland, grassland and forest ecosystems is dissolved and transported along stream networks (Schelsinger and Maleck 1981; Mann and Wetzel 1995). Dissolved organic carbon (DOC) has the potential to both accumulate in the meadow from upstream sources and disseminate downstream (Mann and Wetzel 1995). Synoptic controls like flood or drying events have the potential to stimulate or suppress DOC transport in or out of the meadow surface (Mann and Wetzel 1995). The flux of DOC movement along the stream network was not measured in this study but it is likely to be quite small compared to the larger carbon fluxes between the surface and the atmosphere (Schlesinger and Maleck 1981). A study by Cole et al. (2007) showed that about twice as much carbon enter inland aquatic systems than is released into the oceans, which indicates that a significant amount of DOC is stored in terrestrial ecosystems and/or is turned into a gas and released into the

atmosphere. These processes represent a component of carbon cycling in the meadow but are not likely to have a significant effect on the overall CO₂ budget.

5.3.3 Grazing by Livestock

Grazing animals have a number of ecological impacts on the ecosystem that they occupy. They affect plant community composition, soil characteristics, nitrogen content and the carbon exchange (Jerome et al. 2014). The CO₂ exchange is affected indirectly by biomass consumption, soil compaction, and excretion deposits (Jerome et al. 2014; Allard et al. 2007). They also contribute directly to total ecosystem respiration when they exhale (CO₂) and when they release CH₄ via gastrointestinal processes (Jerome et al. 2014; Allard et al. 2007). In general, the direct effects will have an immediate impact on the CO₂ exchange while the impacts stemming from indirect effects could take multiple years to have a measurable effect on the ecosystem. The magnitude of these effects vary between ecosystem type (LeCain et al. 2002) and management intensity (Allard et al. 2007). Management intensity refers to the stocking rate and both the timing and spatial distribution of the grazing animals. Jerome et al. (2014) found that overgrazing, or having a higher stocking rate than the ecosystem can support, has a negative effect on the ability of the ecosystem to store and sequester CO₂. In general, reducing grazing pressure enhances the ability of ecosystems to sequester and store carbon (LeCain et al. 2002; Allard et al. 2007; Jerome et al. 2014). However, a balanced stocking rate had a negligible effect on the CO₂ exchange.

A herd of about fifty cattle grazed the study site between June and September. The animals began grazing during the peak growth period (Period 2) and continued throughout the remaining observation period. It is unclear whether the stocking rate had a significant effect on the observed CO₂ exchanges. However, the impacts of historic grazing at this site have had a degrading effect on the meadow resulting in channel incision. More studies are needed to accurately quantify the direct and indirect effects of grazing animals on the carbon cycling on meadows and other rangelands.

5.4 Implications for Meadow CO₂ Exchanges under Changing Land-use and Climate

This study and previous research conducted in SN meadows have indicated that water availability shows a strong positive relationship to ecosystem productivity. Channel incision, resulting from degradation, effectively lowers the water table and reduces water available for plants (Kattelmann and Embury 1996; Loheide et al. 2009; Lowry et al. 2011). This process reduces net ecosystem uptake of CO₂. As previously mentioned, we have identified Loney Meadow as “partly” degraded because the vegetation is more consistent with a healthy meadow (Figure 2) than a fully degraded meadow (Figure 3). Despite maintaining an abundant mixture of hydric and mesic plant species, the apparent channel incision may affect the timing and magnitude of seasonal soil moisture levels. If restoration to raise the water is successfully implemented, it has the potential to increase

the carbon uptake providing more soil water for plant roots and to retain high levels of photosynthesis for later in the growing season (Hammersmark et al. 2008).

Similar to the effects of degradation, climate change also has the potential to impact the net CO₂ potential of SN mountain meadows by altering precipitation and seasonal flow patterns (Viers et al. 2013). Research suggests that a warming climate will reduce the amount of precipitation that falls as snow and initiate snowmelt earlier in the season, which will contribute to a longer drier growing season (Loheide et al. 2009; Lowry et al. 2011). Using this study as an example, climate trends suggest that Period 2 (peak growth) would shorten and start earlier and Period 4 (senescence) would lengthen. Since Period 2 accounts for nearly half of the entire net CO₂ uptake measured in the 2016 growing season, a shorter peak growth period would have a significant negative impact on the overall strength of the sink on an annual basis. Similarly, a longer source period, stemming from earlier seasonal drying on the meadow surface, will contribute to a smaller annual sink or, depending on the culminating influences of environmental controls, switch to a net source of CO₂ to the atmosphere. Another potential effect of a warmer climate is increasing soil temperatures, which would likely stimulate higher respiration rates throughout the season. If the high water table is protected it is likely that SN meadows will be more resilient to the effects of climate change and have a greater potential to sequester CO₂ from the atmosphere (Viers and Rheinheimer 2011).

6.0 CONCLUSIONS

This thesis presented results from a study that employed the eddy covariance method to examine surface-atmosphere exchanges of CO₂ in a partly degraded Northern Sierra Nevada meadow. Instrumentation was mounted on a 2.5 m tower and installed near the middle of Loney Meadow for most of the 2016 growing season. The analysis quantified the daily and seasonal surface-atmosphere exchanges of CO₂ and assessed the environmental drivers of this exchange. The results describe the dynamic patterns of productivity over the course of the study period, which provides important information about how the ecosystem functions as well as implications for current and future land use.

On a per square meter basis, Loney Meadow acted as a strong net sink of CO₂ from the atmosphere during the growing phase of the annual cycle. The average daily total flux of CO₂ for the entire study was -7.71 gC m⁻² d⁻¹ and ranged between -18.51 and 2.97 gC m⁻² d⁻¹. Driven by photosynthetically active radiation, the diurnal pattern of NEE closely followed the solar cycle by acting as sink of CO₂ during the day and switching to a source at night. The relationship between available light and growth was much stronger during periods of growth (peak uptake rate of -1 mgC m⁻² s⁻¹) compared to the senescence phases (peak uptake rate of -0.2 mgC m⁻² s⁻¹). However, nocturnal respiration rates ($\sim 0.1 < \text{NEE} < 0.3 \text{ mgC m}^{-2} \text{ s}^{-1}$) were similar across all four seasonal periods.

Following the snowmelt in spring, the seasonal pattern of NEE showed a sharp increase in the uptake of CO₂ until it plateaued in June, which indicated that vegetation density had reached its maximum. With daily total values ranging between about 10 and 50 gC m⁻² d⁻¹, GPP showed a great deal of variability throughout the study period, governed by both light and water availability. RE rates were much smaller and more consistent throughout the growing season compared to GPP. Decline in soil moisture appeared to be the strongest control on the seasonal growth cycle. Dropping soil moisture levels in early July stimulated an increase in NEE, which became positive in August when most of the vegetation had fully senesced.

The annual CO₂ budget for Loney Meadow in 2016 was estimated to be about -222 gC m⁻² y⁻¹. Depending on the magnitude of unmeasured CO₂ fluxes, this annual budget estimate could range between -268 and -61 gC m⁻² y⁻¹. The annual CO₂ budget is likely to vary quite a lot based on interannual climate conditions and across different meadow classifications and elevations. The observed CO₂ exchanges in Loney Meadow showed more similarity to wetlands (Lund et al. 2010; Knox et al. 2015) than most grasslands (Gilmanov et al. 2007). The mountain meadow functioned as a much larger sink of CO₂ from the atmosphere on an annual basis compared to grassland ecosystems, which is attributable to greater water availability via ground water and surface flows. This study supports existing research (Lowry et al. 2011; Viers and Rheinheimer 2011; Blankinship and Hart 2014) that seasonal growth patterns in healthy SN meadows are sensitive to changes in soil moisture levels and thus vulnerable to the effects of climate

change and land use practices. Therefore, preventing further degradation and restoring degraded meadows has an important secondary effect of reducing greenhouse gas concentrations. Employing land management strategies that maintain the health of SN meadows shows clear potential to protect and enhance hydrological processes that impact downstream communities and help mitigate anthropogenic CO₂ emission. Additional long-term monitoring of the carbon exchange in SN meadows is needed to determine the annual CO₂ budget directly through full annual measurements, explore the interannual variability of the carbon budget due to differences in snow and rainfall and to determine differences in CO₂ exchange between meadows due to elevation and topographic position.

7.0 REFERENCES

- Allard, V., Soussana, J. F., Falcimagne, R., Berbigier, P., Bonnefond, J. M., Ceschia, E., ... & Pinares-Patino, C. (2007) "The role of grazing management for the net biome productivity and greenhouse gas budget (CO_2 , N_2O and CH_4) of semi-natural grassland." *Agriculture, Ecosystems & Environment* 121, no. 1: 47-58.
- Allen, B.H. (1987) "Forest and meadow ecosystems in California." *Rangelands*: 125-128.
- Allen-Diaz, B.H. (1991) "Water table and plant species relationships in Sierra Nevada meadows." *American Midland Naturalist*: 30-43.
- American Rivers. (2012). A Guide for Restoring Functionality to Mountain Meadows of the Sierra Nevada: Technical Memorandum. Stillwater Sciences <http://www.americanrivers.org/assets/pdfs/meadow-restoraton/restoration-analysis.pdf?477ed5>
- Anderson, M. (2016). *Hydroclimate Report Water Year 2015*. California Department of Water Resources. Office of the State Climatologist. Sacramento, CA.
- Aubinet, M., Grelle, A., Ibrom, A., Rannik, Ü., Moncrieff, J., Foken, T., ... & Clement, R. (1999) "Estimates of the annual net carbon and water exchange of forests: the EUROFLUX methodology." *Advances in ecological research* 30: 113-175.
- Aubinet, M., Vesala T., and Papale D., eds. (2012). *Eddy covariance: a practical guide to measurement and data analysis*. Springer Science & Business Media.
- Baldocchi, D.D. (2003). "Assessing the eddy covariance technique for evaluating carbon dioxide exchange rates of ecosystems: past, present and future." *Global change biology* 9, no. 4: 479-492.
- Baldocchi, D.D. (2008). "'Breathing' of the terrestrial biosphere: lessons learned from a global network of carbon dioxide flux measurement systems." *Australian Journal of Botany* 56, no. 1: 1-26.
- Baldocchi, D., & Valentini, R. (2004). "Geographic and temporal variation of

- carbon exchange by ecosystems and their sensitivity to environmental perturbations." *SCOPE-SCIENTIFIC COMMITTEE ON PROBLEMS OF THE ENVIRONMENT INTERNATIONAL COUNCIL OF SCIENTIFIC UNIONS* 62: 295-316.
- Blankinship, J.C., & Hart, S.C. (2014). "Hydrological control of greenhouse gas fluxes in a sierra Nevada subalpine meadow." *Arctic, Antarctic, and Alpine Research* 46, no. 2: 355-364.
- Burba, G. (2013). *Eddy covariance method for scientific, industrial, agricultural and regulatory applications: A field book on measuring ecosystem gas exchange and areal emission rates*. LI-Cor Biosciences.
- Castellví, F., & Oliphant, A.J. (2017). "Daytime sensible and latent heat flux estimates for a mountain meadow using in-situ slow-response measurements." *Agricultural and Forest Meteorology* 236: 135-144.
- Cole, J. J., Prairie, Y. T., Caraco, N. F., McDowell, W. H., Tranvik, L. J., Striegl, R. G., ... & Melack, J. (2007) "Plumbing the global carbon cycle: integrating inland waters into the terrestrial carbon budget." *Ecosystems* 10, no. 1: 172-185.
- Crawford, B., Grimmond, C. S. B., & Christen, A. (2011) "Five years of carbon dioxide fluxes measurements in a highly vegetated suburban area." *Atmospheric Environment* 45, no. 4: 896-905.
- Debinski, D. M., Wickham, H., Kindscher, K., Caruthers, J. C., & Germino, M. (2010). "Montane meadow change during drought varies with background hydrologic regime and plant functional group." *Ecology* 91, no. 6: 1672-1681.
- Dong, G., Guo, J., Chen, J., Sun, G., Gao, S., Hu, L., & Wang, Y. (2011) "Effects of spring drought on carbon sequestration, evapotranspiration and water use efficiency in the Songnen meadow steppe in northeast China." *Ecohydrology* 4, no. 2: 211-224.
- Dugas, W. A., Heuer, M. L., & Mayeux, H. S. (1999) "Carbon dioxide fluxes over bermudagrass, native prairie, and sorghum." *Agricultural and Forest Meteorology* 93, no. 2: 121-139.
- Dwire, K. A., Kauffman, J. B., & Baham, J. E. (2006) "Plant species distribution in relation to water-table depth and soil redox potential in montane riparian meadows." *Wetlands* 26, no. 1: 131-146.

- Falge, E., Baldocchi, D., Olson, R., Anthoni, P., Aubinet, M., Bernhofer, C., ... & Granier, A. (2001) "Gap filling strategies for defensible annual sums of net ecosystem exchange." *Agricultural and forest meteorology* 107, no. 1: 43-69.
- Fites-Kaufman, J. A., Rundel, P., Stephenson, N., & Weixelman, D. A. (2007) "Montane and subalpine vegetation of the Sierra Nevada and Cascade ranges." *Terrestrial Vegetation of California. University of California Press, Berkeley:* 456-501.
- Flanagan, Lawrence B., Linda A. Wever, and Peter J. Carlson. (2002) "Seasonal and interannual variation in carbon dioxide exchange and carbon balance in a northern temperate grassland." *Global Change Biology* 8, no. 7: 599-615.
- Foken, T., Aubinet, M., Finnigan, J. J., Leclerc, M. Y., Mauder, M., & Paw U, K. T. (2011) "Results of a panel discussion about the energy balance closure correction for trace gases." *Bulletin of the American Meteorological Society* 92, no. 4: ES13-ES18.
- Gilmanov, T. G., Tieszen, L. L., Wylie, B. K., Flanagan, L. B., Frank, A. B., Haferkamp, M. R., ... & Morgan, J. A. (2005) "Integration of CO₂ flux and remotely sensed data for primary production and ecosystem respiration analyses in the Northern Great Plains: Potential for quantitative spatial extrapolation." *Global Ecology and Biogeography* 14, no. 3: 271-292.
- Gilmanov, T. G., Soussana, J. F., Aires, L., Allard, V., Ammann, C., Balzarolo, M., ... & Cescatti, A. (2007) "Partitioning European grassland net ecosystem CO₂ exchange into gross primary productivity and ecosystem respiration using light response function analysis." *Agriculture, ecosystems & environment* 121, no. 1: 93-120.
- Gilmanov, T. G., Aires, L., Barcza, Z., Baron, V. S., Belletti, L., Beringer, J., ... & Cook, D. (2010). "Productivity, respiration, and light-response parameters of world grassland and agroecosystems derived from flux-tower measurements." *Rangeland ecology & management* 63, no. 1: 16-39.
- Goulden, M. L., Munger, J. W., FAN, S. M., Daube, B. C., & Wofsy, S. C. (1996). "Measurements of carbon sequestration by long-term eddy covariance: Methods and a critical evaluation of accuracy." *Global change biology* 2, no. 3: 169-182.
- Ham, J. M., & Knapp, A. K. (1998). "Fluxes of CO₂, water vapor, and energy from a

- prairie ecosystem during the seasonal transition from carbon sink to carbon source." *Agricultural and Forest Meteorology* 89, no. 1: 1-14.
- Hammersmark, C.T., Mark C.R., and Jeffrey F.M. (2008). "Quantifying the hydrological effects of stream restoration in a montane meadow, northern California, USA." *River Research and applications* 24, no. 6: 735-753.
- Hamlet, A. F., Mote, P. W., Clark, M. P., & Lettenmaier, D. P. (2005). "Effects of temperature and precipitation variability on snowpack trends in the western United States." *Journal of Climate* 18, no. 21: 4545-4561.
- Haugo, R. D., & Halpern, C. B. (2007). "Vegetation responses to conifer encroachment in a western Cascade meadow: a chronosequence approach." *Botany* 85, no. 3: 285-298.
- Holland, R.F. (1986) "Preliminary descriptions of the terrestrial natural communities of California."
- Hsieh, C. I., Katul, G., & Chi, T. W. (2000)."An approximate analytical model for footprint estimation of scalar fluxes in thermally stratified atmospheric flows." *Advances in water Resources* 23, no. 7: 765-772.
- Hutchinson, R. (2016). South Yuba River Citizens League. Personal Communication (email).
- Jérôme, E., Beckers, Y., Bodson, B., Heinesch, B., Moureaux, C., & Aubinet, M. (2014)."Impact of grazing on carbon dioxide exchanges in an intensively managed Belgian grassland." *Agriculture, ecosystems & environment* 194: 7-16.
- Kato, T., Tang, Y., Gu, S., Cui, X., Hirota, M., Du, M., ... & Oikawa, T. (2004)."Carbon dioxide exchange between the atmosphere and an alpine meadow ecosystem on the Qinghai-Tibetan Plateau, China." *Agricultural and forest meteorology* 124, no. 1: 121-134.
- Kattelmann, R. & Embury, M. (1996). "Riparian areas and wetlands." In *Sierra Nevada Ecosystem Project, Final Report to Congress*, vol. 3.
- Kayranli, B., Scholz, M., Mustafa, A., & Hedmark, Å. (2010). "Carbon storage and fluxes within freshwater wetlands: a critical review." *Wetlands* 30, no. 1: 111-124.
- Knox, S. H., Sturtevant, C., Matthes, J. H., Koteen, L., Verfaillie, J., & Baldocchi, D.

- (2015). "Agricultural peatland restoration: effects of land-use change on greenhouse gas (CO₂ and CH₄) fluxes in the Sacramento-San Joaquin Delta." *Global change biology* 21, no. 2: 750-765.
- Kondolf, G. M., Kattelmann, R., Embury, M., & Erman, D. C. (1996). "Status of riparian habitat." In *Sierra Nevada Ecosystem Project: Final report to Congress*, vol. 2, pp. 1009-1030.
- LeCain, D. R., Morgan, J. A., Schuman, G. E., Reeder, J. D., & Hart, R. H. (2002). "Carbon exchange and species composition of grazed pastures and exclosures in the shortgrass steppe of Colorado." *Agriculture, ecosystems & environment* 93, no. 1: 421-435.
- Loheide, S. P., & Gorelick, S. M. (2007). "Riparian hydroecology: a coupled model of the observed interactions between groundwater flow and meadow vegetation patterning." *Water Resources Research* 43, no. 7.
- Loheide, S. P., Deitchman, R. S., Cooper, D. J., Wolf, E. C., Hammersmark, C. T., & Lundquist, J. D. (2009). "A framework for understanding the hydroecology of impacted wet meadows in the Sierra Nevada and Cascade Ranges, California, USA." *Hydrogeology Journal* 17, no. 1 (2009): 229-246.
- Lowry, C. S., Loheide, S. P., Moore, C. E., & Lundquist, J. D. (2011). "Groundwater controls on vegetation composition and patterning in mountain meadows." *Water Resources Research* 47, no. 10.
- Lund, M., Lafleur, P. M., Roulet, N. T., Lindroth, A., Christensen, T. R., Aurela, M., ... & Oechel, W. C. (2010). "Variability in exchange of CO₂ across 12 northern peatland and tundra sites." *Global Change Biology* 16, no. 9: 2436-2448.
- Ma, S., Baldocchi, D. D., Xu, L., & Hehn, T. (2007). "Inter-annual variability in carbon dioxide exchange of an oak/grass savanna and open grassland in California." *Agricultural and Forest Meteorology* 147, no. 3: 157-171.
- Maher, S.C. (2015). "Bio-Micrometeorology of a Sierra Nevada Montane Meadow." Master's Thesis. San Francisco State University.
- Mann, C.J., and Robert G.W. (1995) "Dissolved organic carbon and its utilization in a riverine wetland ecosystem." *Biogeochemistry* 31, no. 2 (1995): 99-120.
- Massman, W. J., & Lee, X. (2002) "Eddy covariance flux corrections and uncertainties in

- long-term studies of carbon and energy exchanges." *Agricultural and Forest Meteorology* 113, no. 1: 121-144.
- Moffat, A. M., Papale, D., Reichstein, M., Hollinger, D. Y., Richardson, A. D., Barr, A. G., ... & Falge, E. (2007). "Comprehensive comparison of gap-filling techniques for eddy covariance net carbon fluxes." *Agricultural and Forest Meteorology* 147, no. 3: 209-232.
- Norton, J. B., Jungst, L. J., Norton, U., Olsen, H. R., Tate, K. W., & Horwath, W. R. (2011). "Soil carbon and nitrogen storage in upper montane riparian meadows." *Ecosystems* 14, no. 8: 1217-1231.
- NRCS (Natural Resources Conservation Service). (2017). United States Department of Agriculture. Retrieved from: <https://www.wcc.nrcs.usda.gov/snow/>
- Oke, T. R. (1987). "Boundary layer climates. 2nd." *Methuen, 289p.*
- Oliphant, A. J., D. Dragoni, B. Deng, C. S. B. Grimmond, H-P. Schmid, and S. L. Scott. "The role of sky conditions on gross primary production in a mixed deciduous forest." *Agricultural and forest meteorology* 151, no. 7 (2011): 781-791.
- Oliphant, A.J. (2012) "Terrestrial Ecosystem-Atmosphere Exchange of CO₂, Water and Energy from FLUXNET; Review and Meta-Analysis of a Global in-situ Observatory." *Geography Compass* 6, no. 12 (2012): 689-705.
- Papale, D., Reichstein, M., Aubinet, M., Canfora, E., Bernhofer, C., Kutsch, W., ... & Yakir, D. (2006). "Towards a standardized processing of Net Ecosystem Exchange measured with eddy covariance technique: algorithms and uncertainty estimation." *Biogeosciences* 3, no. 4: 571-583.
- Pope, K. L., Montoya, D. S., Brownlee, J. N., Dierks, J., & Lisle, T. E. (2015). "Habitat conditions of montane meadows associated with restored and unrestored stream channels of California." *Ecological Restoration* 33, no. 1: 61-73.
- Purdy, S. E., Moyle, P. B., Fish, M., Wilson, D., Baker, B., Stead, J., ... & Mantallica, E. (2006). "Mountain Meadows of the Sierra Nevada An integrated means of determining ecological condition in mountain meadows Protocols and Results from 2006."
- Ratliff, R.D. (1982) "A meadow site classification for the Sierra Nevada, California."

- Ratliff, R.D. (1985) "Meadows in the Sierra Nevada of California: state of knowledge."
- Schlesinger, W. H., & Melack, J. M. (1981). Transport of organic carbon in the world's rivers. *Tellus*, 33(2), 172-187.
- Schmid, H. P., Grimmond, C. S. B., Cropley, F., Offerle, B., & Su, H. B. (2000). Measurements of CO₂ and energy fluxes over a mixed hardwood forest in the mid-western United States. *Agricultural and Forest Meteorology*, 103(4), 357-374.
- Scott, R. L., Hamerlynck, E. P., Jenerette, G. D., Moran, M. S., & Barron-Gafford, G. A. (2010). Carbon dioxide exchange in a semidesert grassland through drought-induced vegetation change. *Journal of Geophysical Research: Biogeosciences*, 115(G3).
- Stewart, I. T., Cayan, D. R., & Dettinger, M. D. (2005). Changes toward earlier streamflow timing across western North America. *Journal of climate*, 18(8), 1136-1155.
- Stoy, P. C., Katul, G. G., Siqueira, M. B., Juang, J. Y., Novick, K. A., Uebelherr, J. M., & Oren, R. (2006). An evaluation of models for partitioning eddy covariance-measured net ecosystem exchange into photosynthesis and respiration. *Agricultural and Forest Meteorology*, 141(1), 2-18.
- Stoy, P. C., Mauder, M., Foken, T., Marcolla, B., Boegh, E., Ibrom, A., ... & Cescatti, A. (2013). A data-driven analysis of energy balance closure across FLUXNET research sites: The role of landscape scale heterogeneity. *Agricultural and Forest Meteorology*, 171, 137-152.
- Suyker, A. E., & Verma, S. B. (2001). Year-round observations of the net ecosystem exchange of carbon dioxide in a native tallgrass prairie. *Global Change Biology*, 7(3), 279-289.
- Svejcar, T., Angell, R., Bradford, J. A., Dugas, W., Emmerich, W., Frank, A. B., ... & Mielnick, P. (2008). Carbon fluxes on North American rangelands. *Rangeland Ecology & Management*, 61(5), 465-474.
- SYRCL (South Yuba River Citizens League). (2017) Retrieved from:
<http://yubariver.org/our-work/river-education/interpretive-trails/loney-meadow-interpretive-trail/>

- Viers, J. H., & Rheinheimer, D. E. (2011). Freshwater conservation options for a changing climate in California's Sierra Nevada. *Marine and Freshwater Research*, 62(3), 266-278.
- Viers, J. H., Purdy, S. E., Peek, R. A., Fryjoff-Hung, A., Santos, N. R., Katz, J. V., ... & Yarnell, S. M. (2013). Montane Meadows In The Sierra Nevada.
- Weixelman, D. A., Hill, B., Cooper, D. J., Berlow, E. L., Viers, J. H., Purdy, S. E., ... & Gross, S. E. (2011). A field key to meadow hydrogeomorphic types for the Sierra Nevada and southern Cascade Ranges in California. *US Forest Service, Pacific Southwest Region, Vallejo, California, USA*.
- Wilson, K., Goldstein, A., Falge, E., Aubinet, M., Baldocchi, D., Berbigier, P., ... & Grelle, A. (2002). Energy balance closure at FLUXNET sites. *Agricultural and Forest Meteorology*, 113(1), 223-243.
- WRCC (Western Regional Climate Center). (2017). Retrieved from:
<https://wrcc.dri.edu/cgi-bin/cliMAIN.pl?ca1018>
- Wohlfahrt, G., Anfang, C., Bahn, M., Haslwanter, A., Newesely, C., Schmitt, M., ... & Cernusca, A. (2005). Quantifying nighttime ecosystem respiration of a meadow using eddy covariance, chambers and modelling. *Agricultural and Forest Meteorology*, 128(3), 141-162.
- Wohlfahrt, G., Hammerle, A., Haslwanter, A., Bahn, M., Tappeiner, U., & Cernusca, A. (2008). Seasonal and interannual variability of the net ecosystem CO₂ exchange of a temperate mountain grassland: Effects of weather and management. *Journal of Geophysical Research: Atmospheres*, 113(D8).
- Xu, L., & Baldocchi, D. D. (2004). Seasonal variation in carbon dioxide exchange over a Mediterranean annual grassland in California. *Agricultural and Forest Meteorology*, 123(1), 79-96.